Laboratory Assessment of the Impact of Chemical Oxidation, Mineral Dissolution, and Heating on the Nitrogen Isotopic Composition of Fossil-bound Organic Matter

Alfredo Martínez-García*[1], Jonathan Jung[1], Xuyuan E. Ai[1,2], Daniel M. Sigman[2], Alexandra Auderset[1], Nicolas Duprey[1], Alan Foreman[1], François Fripiat[1,3], Jennifer Leichliter[1], Tina Lüdecke [1], Simone Moretti[1], Tanja Wald[1]

[1] *Max Planck Institute for Chemistry, Mainz, Germany*

[2] *Princeton University, Princeton, USA*

[3] *Université Libre de Bruxelles, Brussels, Belgium*

*corresponding author: Alfredo Martínez-García (a.martinez-garcia@mpic.de)

Key Points:

- Fossil-bound organic matter is well protected by the mineral matrix from chemical changes in the surrounding environment.
- Partial dissolution of fossil calcite, aragonite, opal, and enamel has a negligible effect on their N isotopic composition and N content.
- During heating, fossil N content and isotopic composition remains unchanged if the structure of the inorganic matrix is not compromised.

Abstract

Fossil-bound organic material holds great potential for the reconstruction of past changes in nitrogen (N) cycling. Here, with a series of laboratory experiments, we assess the potential effect of oxidative degradation, fossil dissolution, and thermal alteration on the fossil-bound N isotopic composition of different fossil types, including deep and shallow water scleractinian corals, foraminifera, diatoms and tooth enamel. Our experiments show that exposure to different oxidizing reagents does not significantly affect the N isotopic composition or N content of any of the fossil types analyzed, demonstrating that organic matter is well protected from changes in the surrounding environment by the mineral matrix. In addition, we show that partial dissolution (of up to 70-90%) of fossil aragonite, calcite, opal, or enamel matrixes has a negligible effect on the N isotopic composition or N content of the fossils. These results suggest that the isotopic composition of fossil-bound organic material is relatively uniform, and also that N exposed during dissolution is lost without significant isotopic discrimination. Finally, our heating experiments show negligible changes in the N isotopic composition and N content of all fossil types at 100 ºC. At 200 ºC and hotter, the N loss and associated nitrogen isotope changes appear to be directly linked to the sensitivity of the mineral matrix to thermal stress. These results suggest that, so long as high temperature does not compromise the mineral structure, the biomineral matrix acts as a closed system with respect to N, and the N isotopic composition of the fossil remains unchanged.

Plain Language Summary

The ratio of the heavy and light isotopes of nitrogen (^{15}N and ^{14}N) in the organic material contained within the mineral structure of fossils can be used to reconstruct past changes in biological and chemical processes. With a series of laboratory experiments, we evaluate the potential effects of chemical conditions, fossil dissolution, and heating on the nitrogen isotopic composition ($^{15}N/^{14}N$ ratio) of corals, foraminifera, diatoms and tooth enamel. Our results indicate that these processes do not have a significant effect on the $^{15}N/^{14}N$ of fossils, suggesting that the mineral matrix provides a barrier that isolates a fossil's organic nitrogen from the surrounding environment, preventing alteration of its $^{15}N/^{14}N$. In addition, we show that if part of the fossil-bound organic nitrogen is exposed by dissolution or heating, it is lost without affecting the $^{15}N/^{14}N$ of the organic material that remains in the mineral. These findings imply that the

original $^{15}N/^{14}N$ ratio incorporated by the organism is preserved in the geologic record. Therefore, measurements of the nitrogen isotopes on fossils can provide faithful biological, ecological, and environmental information about the past.

1 Introduction

The stable isotopes of nitrogen (^{14}N and ^{15}N) can offer important insights into present and past changes in the cycling of this key element through organisms, food webs, and environments (Casciotti, 2016; Deniro and Epstein, 1981; Fripiat et al., 2021; Sigman and Fripiat, 2019; Straub et al., 2021; Wolf et al., 2009). Their use in paleo-reconstructions requires the development of faithful geochemical archives that are unaffected by diagenetic alteration and/or contamination by exogenous N. In recent years, the analysis of the N isotopic composition of the organic matter bound within the mineral structure of fossil skeletons (e.g., foraminifera, corals, diatoms, otoliths and tooth enamel) has emerged as a promising archive of the original isotopic signature of the organism that is protected from degradation for thousands to millions of years (Ai et al., 2020; Altabet and Curry, 1989; Auderset et al., in press; Duprey et al., 2020; Erler et al., 2020; Erler et al., 2016; Farmer et al., 2021; Kast et al., 2019; Leichliter et al., 2021; Lueders-Dumont et al., 2018; Martinez-Garcia et al., 2014; Ren et al., 2017; Ren et al., 2009; Robinson et al., 2004; Robinson et al., 2005; Shemesh et al., 1993; Sigman et al., 1999; Sigman et al., 2021; Straub et al., 2013; Studer et al., 2021; Studer et al., 2015; Studer et al., 2018; Wang et al., 2014; Wang et al., 2016; Wang et al., 2017).

The compounds that comprise fossil-bound organic matter play an active, but still poorly understood, physiological role in the biomineralization process. In planktonic foraminifera and stony corals, this organic matter consists of a series of proteins and polysaccharides that regulate the calcification process (Cusack and Freer, 2008; Ingalls et al., 2003; Weiner and Erez, 1984), with recent suggestions of a lipid component as well (Swart et al., 2021). In enamel, a series of specific proteins (amelogenin, enamelin, amelotin, and ameloblastin) play a key role as the structural scaffolds that determine mineral morphology during enamel development (Bai et al., 2020; Castiblanco et al., 2015). Although most of these organic compounds are digested and removed at the enamel maturation stage to achieve maximum hardness, these specific proteins are still found in tooth enamel samples that are millions of years old (Cappellini et al., 2019). In diatoms, frustule-bound organic matter is composed mainly of a set of taxon-specific polyamines

and silaffins that promote silica precipitation during the formation of the diatom frustule (Bridoux et al., 2012a; Bridoux et al., 2012b; Kroger, 2002; Kroger et al., 2000). Fossil-bound organic material is, therefore, native to the organism.

Several lines of evidence suggest that the mineral matrix provides an effective barrier that protects the native, fossil-bound organic matter from contamination by external organic material from the surrounding sedimentary environment. For example, the amino acid composition of fossil-bound organic matter has significant differences from cooccurring organic matter in the sedimentary environment. The non-proteinogenic amino acids β-alanine and γ-aminobutyric are formed by microbial decarboxylation of aspartic and glutamic acids, making them ubiquitously abundant in marine sediments (Cowie and Hedges, 1994; Dauwe and Middelburg, 1998; Whelan, 1977). Thus, the absence of these amino acids in foraminifera tests suggests that the mineral matrix provides an effective barrier against microbial attack of fossil-bound organic matter and prevents the exchange of compounds with the surrounding sediments (Schroeder, 1975). In addition, laboratory studies indicate that the racemization reaction proceeds without significant impact on the nitrogen and carbon isotopic composition of the L- and D-enantiomers, so that the isotopic comparison of the enantiomers can be used to assess contamination of fossil-bound organic material (Engel and Macko, 1986). For example, the similarity of the carbon isotopic compositions of the D and L enantiomers of several individual amino acids in late Pleistocene land snail shells confirmed that their shell-bound amino acids were endogenous to the fossil (Engel et al., 1994). Finally, new biochemical and molecular biological tools are beginning to be applied to fossil-bound organic matter and speak to its fossil-native origin. For example, a recent analysis a 1.77 Ma extinct Rhinoceros tooth has shown that its enamel proteome is endogenous and almost complete (Cappellini et al., 2019).

The issue of endogeneity aside, there is also the possibility of effects of oxidative degradation, mineral dissolution, and thermal alteration on the N isotopic composition of fossil-bound organic material. Chemical and biological degradation are common in marine sediments and other environments (Arndt et al., 2013) and can alter substantially the original nitrogen isotopic composition of sedimentary organic matter (Robinson et al., 2012). A key postulate in the application of the fossil-bound N isotope method is that the mineral matrix provides an effective

physical barrier that isolates organic compounds from the surrounding environment, protecting them from both external contamination and chemical or biological attack. The relative stability of the N content per mg of mineral of different fossil types (e.g., planktonic foraminifera, diatoms, scleractinian corals and tooth enamel) of the same species/genus over thousands and even millions of years supports this postulate (Auderset et al., in press; Kast et al., 2019; Leichliter et al., 2021; Ren et al., 2017; Studer et al., 2012; Wang et al., 2017). However, the stability of the N isotopic composition in response to changes in external chemical conditions that could favor organic matter degradation has not been systematically assessed.

Dissolution of calcium carbonate and opal is a widespread phenomenon in the ocean and other sedimentary systems (Sulpis et al., 2021; Van Cappellen et al., 2002). Partial dissolution of fossil mineral structures can substantially impact many geochemical proxies that rely on the isotopic and/or elemental composition of the inorganic biomineral matrix. These effects are thought to derive largely from the preferential dissolution of parts of the biomineral that have a distinct elemental/isotopic composition (Brown and Elderfield, 1996; McCorkle et al., 1995; Pearson, 2017; Rosenthal et al., 2000; Smith et al., 2016). In contrast, dissolution is thought to have a minimal effect on the N isotopic composition of organic matter bound within the biomineral structure of the fossils because: (i) the organic matter exposed after dissolution should ultimately be degraded and/or removed during cleaning prior to analysis (see section 2.3), and (ii) no reason is known for the isotopic composition of fossil-bound organic matter to vary coherently with dissolution susceptibility across the biomineral structure (Smart et al., 2018). However, so far, these two arguments have not been tested.

In addition, sedimentary organic matter degradation can increase during burial as a consequence of the temperature rise associated with local geothermal gradients, potentially causing important impacts on its molecular and isotopic composition (Burdige, 2006). Although typical thermal gradients in Cenozoic marine sediments are relatively small (< 60 ºC) (Malinverno and Martinez, 2015), they can be substantially larger (> 500 ºC) in other depositional settings that contain identifiable fossils (Rejebian et al., 1987). In any case, the potential effect of thermal degradation on the nitrogen isotopic composition of fossil-bound organic matter has not been examined.

In this study, we report results from laboratory experiments designed to evaluate the potential effects of oxidizing conditions, mineral dissolution, and thermal alteration on the nitrogen isotopic composition of fossil-bound organic matter.

2 Materials and Methods

2.1 Sample Materials

The different experiments were performed using a series of sample materials prepared at the Max Plank Institute for Chemistry (MPIC) in Mainz, Germany. These materials are intended to be representative of different fossil types typically used in paleo-reconstructions (Table 1) and include: modern deep-sea (*Lophelia pertusa, LO-1*) and shallow water (*Porites sp., PO-1*) coral samples; late Holocene mixed foraminifera fractions (63-315 μm) from sediment cores collected in the North Atlantic (MF-1) and the Southern Ocean (MF-2); modern tooth enamel from an African elephant (*Loxodonta africana,* AG-Lox); fossil enamel from a Pleistocene (ca. 2.5 to 2.3 Ma) suid (*Notochoerus scotti*, Noto-2) from Zone 3A-2 of the Chiwondo Beds in Malawi (prepared from the same tooth as "Noto-1" reported in Leichliter et al. (2021)); fossil enamel from a Plio-Pleistocene (ca. 3.75 to 1.8 Ma) hippopotamus (*Hippopotamus amphibious,* Hippo-1) from Unit 3 at the Chiwondo Beds in Malawi; and two diatom samples obtained from sediment cores from the Antarctic Zone of the Southern Ocean (DI-1 and DI-2) prepared following the diatom separation methods described in (Studer et al., 2015) .

Table 1. Description of the sample materials analyzed in this study

MPIC-ID	Description/Genus/Species	Matrix	Location	Age	Reference
MF-1	Mixed Foraminifera, 63-315 μm size fraction	Calcite	North Atlantic	Late Holocene	*This study*
MF-2	Mixed Foraminifera, 63-315 μm size fraction	Calcite	Southern Ocean	Late Holocene	*This study*
PO-1	*Porites sp.*	Aragonite	Chuuk, Micronesia	Modern	*(Leichliter et al., 2021)*
LO-1	*Lophelia pertusa*	Aragonite	North Atlantic	Modern	*(Leichliter et al., 2021)*
AG-Lox	*Loxodonta africana*	Enamel	Africa	Modern	*(Gehler et al., 2012; Leichliter et al., 2021)*
Noto-2	*Notochoerus scotti*	Enamel	Malawi, Africa	2.3 - 2.5 Ma	*(Kullmer, 2008; Leichliter et al., 2021)*

Hippo-1	*Hippopotamus amphibius*	Enamel	Malawi, Africa	1.8- 3.75 Ma	*This study*
DI-1	Diatoms, < 63um size fraction	Opal	Southern Ocean, core PS75/72-2	MIS11 (374-424 ka)	*This study*
DI-2	Diatoms, < 63um size fraction	Opal	Southern Ocean, core PS69/899-2	MIS 5 (120-124 ka)	*This study*

2.2 Experimental design

The experimental design is summarized in Fig. 1, and the different steps followed in each experiment are described below and in the next sections. For each sample type, an aliquot of uncleaned powder was taken and used in our chemical oxidation experiment. The remaining powder was subsequently cleaned in four aliquots (of 50 mg each) following the reductive-oxidative cleaning methods described in Section 2.3. After cleaning, the dry fossil powder was combined in a single vial and homogenized. This homogenous cleaned powder was measured (at least in triplicate) and used as a control sample for all our treatments. For both the dissolution and the thermal degradation experiments, samples were measured twice: (1) directly after the treatment, and (2) with a recleaning of the fossil powders after the dissolution and temperature treatments.

Each treatment was performed in triplicate for all the fossil standards described in Table 1. We performed a total of 413 individual measurements. The results of the experiments are reported in Figures 2 to 5 and the data are available in the Supporting Information file.

2.2.1 Chemical oxidation experiment

We designed an experiment in which the different fossil standard samples (Table 1) were exposed to consecutive oxidative cleaning steps using a solution of sodium hypochlorite (corals), basic potassium persulfate (foraminifera and tooth enamel), and perchloric acid (diatoms), following the methods described in Section 2.3. The first oxidation step had the objective of removing any external (non-mineral-bound) organic material and is part of our standard cleaning procedure. The second oxidation step was used to evaluate the potential effect of exposure to strongly oxidizing conditions on the N content and isotopic composition of the remaining fossil-bound organic matter. If the mineral matrix provides an effective barrier against chemical attack, we would expect to see no change in N content or $\delta^{15}N$ when comparing the first and second

oxidative cleanings. In contrast, if the matrix is permeable, the organic matter would be vulnerable to chemical attack, and we would expect a decrease in N content. In addition, if this process preferentially removes ^{14}N or ^{15}N, we would expect a change in $\delta^{15}N$ and a decrease in N content. In contrast, if the mineral matrix is permeable but organic material is removed without any isotopic discrimination, we would expect to find a decrease in N content but no change in $\delta^{15}N$.

2.2.2 Mineral Dissolution Experiment

Artificial dissolution experiments of the calcite (foraminifera), aragonite (corals) and enamel (teeth) standards were performed by adding different amounts of HCl to known quantities of the standard mineral powder. We tested three treatments that resulted in around 25%, 50% and 70% dissolution in corals and foraminifera, and in around 40%, 60% and 75-90% dissolution in enamel (Fig. 2). Each treatment was performed in triplicate for each standard fossil material. After dissolution, the remaining powder was rinsed five times with Milli-Q water and dried in a clean oven at 60 ºC. The dry powder was weighed and its N isotopic composition was determined using the methods described in Section 2.3. We compared the results obtained when measuring the samples directly after dissolution to those obtained when the samples were recleaned after the dissolution treatment, in order to evaluate the possibility that organic matter was exposed during the dissolution but not removed during the rinsing with Milli-Q water.

For the diatom dissolution experiment, ~15-25 mg aliquots of cleaned diatom standard material were placed in pre-combusted 4 ml glass vials and filled with 4 ml 0.15 M NaOH solution. The vials were then placed in an 85 °C water bath for ~15 min (~40% dissolution), ~1 hr (~60% dissolution), and 1.5 hr (70% dissolution). In the 70% dissolution experiment, the supernatant was replaced with fresh 0.15 M NaOH solution after one hour and the samples were placed back in 85 °C water bath for another 0.5 hr. In all experiments, the supernatant was discarded after heating, and the residual opal samples were rinsed 5 times with Milli-Q water and dried in a clean oven at 60 °C for 36 hours. N isotopic composition was determined using the methods described in Section 2.3.

The aim of these experiments was to compare the potential effects of partial dissolution of the inorganic mineral matrix on the isotopic composition of fossil-bound organic matter. If the organic matter is uniformly distributed and is completely removed after dissolution, we would expect to see no change in N content or $\delta^{15}N$. In contrast, if the isotopic composition of the organic N within the fossil is heterogenous and dissolution preferentially affects parts of the fossil with a distinct isotopic composition or N concentration, we would expect to see differences in $\delta^{15}N$ and/or N content between the different treatments and the untreated control sample. Likewise, if organic matter is exposed during dissolution, but not removed during washing, we could see an increase in N content. However, this additional N should be removed if the samples are oxidatively cleaned after dissolution. If there are no differences in $\delta^{15}N$ between the samples that are oxidatively cleaned after dissolution and the ones that are not, we could conclude that the exposure of organic matter does not alter its isotopic composition.

2.2.3 Thermal degradation experiment

We performed a series of laboratory experiments in which the cleaned diatom, coral, foraminifera and tooth enamel samples described in Table 1 were exposed to different temperatures (100 ºC, 200 ºC, 300 ºC, 400 ºC and 500 ºC) in a muffle furnace for 24 hours. Aliquots of the different standard materials were placed in the muffle furnace inside 4 ml pre-combusted glass vials covered with pre-combusted aluminum foil. The muffle furnace was heated from room temperature to the target temperature in 1.5 hours and kept at temperature for 24 hours. Then, the furnace was allowed to cool down to a temperature below 50 °C before the sample vials were taken out of the furnace. The N isotopic composition of the remaining diatom, coral, foraminifera, and tooth enamel powder was measured following the procedure described in Section 2.3. Similar to the dissolution experiment described in the previous section, we compared the results obtained when measuring the samples directly after heating to those obtained when the samples were recleaned after the heating treatment.

The aim of these experiments was to compare the potential effects of thermal degradation of fossil-bound organic matter on its isotopic composition. If fossil-bound organic matter is not altered during heating, we would expect to see no change in N content or $\delta^{15}N$ with increasing temperature. However, if the thermal degradation of fossil-bound organic matter is incomplete

and affects preferentially a fraction of organic matter with a specific isotopic composition, we would expect a change in both N content and isotopic composition. In contrast, if the fraction of fossil-bound organic matter that is affected by heating is completely combusted, we would expect to find a decrease in N content, but no substantial change in isotopic composition. Finally, if there are no differences in N content and $\delta^{15}N$ between the samples that are oxidatively cleaned after heating and the ones that are not, we could conclude that the exposed organic material is completely combusted.

2.3 Analysis of fossil-bound nitrogen isotopes

The analyses were performed in the laboratories of the Organic Isotope Geochemistry Group of the Department of Climate Geochemistry at the MPIC. The nitrogen isotopic composition (expressed as $\delta^{15}N = (((^{15}N/^{14}N)_{sample}/(^{15}N/^{14}N)_{air} - 1) * 1000)$ of the samples was determined using the oxidation-denitrifier method (Knapp et al., 2005). Prior to analysis, sample powders were chemically cleaned following standard reductive and oxidative cleaning steps that have been described previously for each fossil type (Leichliter et al., 2021; Ren et al., 2009; Studer et al., 2015; Wang et al., 2014), as described below.

The reductive cleaning step was the same for all fossil types. 50 mg of powdered fossil samples were weighed into 15 ml polypropylene centrifuge tubes, and 7 ml of sodium bicarbonate-buffered dithionite citrate solution (Mehra and Jackson, 1958) was added to the samples. The tubes were then placed in a 80 ºC water bath for ten minutes. This step was originally included to remove metal oxide coatings, which could potentially trap exogenous nitrogen (Mehra and Jackson, 1958; Ren et al., 2009). After cooling, samples were centrifuged, the solution was decanted, and the remaining powder was rinsed three times with 10 ml of Milli-Q water (18.2 MΩ cm, < 5 ppm TOC) and transferred to pre-combusted 4 ml glass vials.

Following our standard protocols, the oxidative cleaning was performed using re-crystalized potassium persulfate for foraminifera and enamel material, sodium hypochlorite for coral samples, and perchloric acid for diatom samples. In the first protocol, a basic potassium persulfate solution consisting of 2 g of sodium hydroxide, 2 g of potassium persulfate and 100 ml of Milli-Q water was added to the foraminifera and enamel samples, which were subsequently

292 autoclaved for 65 minutes at 120 ºC. The oxidative solution was removed by aspiration after
293 centrifugation, and the remaining powder was rinsed four times with 4 ml Milli-Q water and
294 dried in a clean oven at 60 ºC for 24 hours. In the second protocol, coral samples were soaked in
295 4.25 ml sodium hypochlorite (10–15% available chlorine), in pre-combusted glass vials placed
296 horizontally on a shaker table rotating at 120 rpm for 24 h. Samples were then centrifuged, the
297 solution was removed by aspiration, and the remaining powder was rinsed three times with Milli-
298 Q water and dried in a clean oven at 60 ºC for 24 hours. In the third protocol, diatoms were
299 cleaned with 7% perchloric acid in a boiling water bath for 1 hour in 15 ml polypropylene
300 centrifuge tubes, centrifuged and decanted. The remaining powder was transferred to pre-
301 combusted 40 ml glass tubes and subsequently cleaned with 60% perchloric acid in boiling water
302 bath for 2 hours, rinsed with Milli-Q water until the pH was neutral, and dried for 24-48 hours in
303 a clean oven at 60 °C.
304
305 After cleaning, foraminifera, coral and enamel powder were demineralized using 4 *N*
306 hydrochloric acid, and organic N was oxidized to nitrate with a solution prepared using 0.7 g
307 recrystallized potassium persulfate, 4 ml of 6.25 *N* NaOH, and 95 ml Milli-Q water. Samples
308 were autoclaved for 65 min at 120 °C, and centrifuged. Cleaned diatoms were dissolved and the
309 organic N released from the frustules oxidized to nitrate in one step by adding 1 ml of a solution
310 prepared using 3 g of recrystallized potassium persulfate, 12 ml of 6.25 N NaOH, and 83 ml
311 Milli-Q water. Diatom samples were autoclaved at 120 °C for 95 min. For all fossil types
312 analyzed, the concentration of nitrate in the oxidized solutions was determined by
313 chemiluminescence (Braman and Hendrix, 2002). An aliquot of the nitrate solution equivalent to
314 5 nmol of N was quantitatively converted to nitrous oxide (N_2O) using the denitrifier method
315 (Sigman et al., 2001), and the $\delta^{15}N$ of the N_2O generated was determined by a purpose-built inlet
316 system coupled to a Thermo MAT253 Plus stable isotope ratio mass spectrometer (Weigand et
317 al., 2016).
318
319 International reference nitrate standards (USGS34, IAEA-NO-3) were analyzed with each batch
320 of samples and used to calculate nitrogen concentration and calibrate the isotopic composition of
321 samples *vs.* air N_2. The N content and $\delta^{15}N$ of the persulfate oxidation reaction blank was
322 measured in duplicate in each batch of samples and was used to correct the fossil-bound

measurements. International reference amino acid standards (USGS40 and USGS41 or USGS65) were analyzed to monitor the persulfate oxidation. The N content of the blank across the different batches was between 0.1 and 0.4 nmol/ml. The precision (1σ) for repeated $\delta^{15}N$ measurements of the control standards described in Section 2.1 was 0.10‰ for the MF-1 foraminifera standard (n=9), 0.16‰ for the MF-2 standard (n=9), 0.10‰ for the LO-1 coral standard (n=9), 0.17‰ for the PO-1 coral standard (n=9), 0.11‰ for the AG-Lox tooth standard (n=6), 0.28‰ for the Noto-2 tooth standard (n=3), 0.68‰ for the Hippo-1 standard (n=3), and 0.02‰ for the DI-1 diatom standard (n=3).

2.4 Statistical analysis

The results of the multiple measurements for each treatment in the different experiments are presented as means ±1 standard deviation (panels A and B in Figs. 2 to 4, and E and F in Figs. 3 and 4, and all panels in Fig. 5). When calculating the difference between the control and the treatment, the standard deviations of the two measurements were propagated (panels C and D in Figs. 2 to 4, and G and H in Figs 3 and 4). The mean $\delta^{15}N$ values obtained after the different treatments were compared to those obtained for the untreated control sample with a Student's t-test. A p-value of < 0.01 was considered statistically significant in the discussion, p-values are reported in the Supporting Information.

3 Results and Discussion

3.1 Impact of chemical oxidation on fossil-bound $\delta^{15}N$

Relative to the uncleaned sample, our experiments showed a significant decrease in N content during the first oxidative cleaning in all the fossils analyzed, except in the diatom sample (Fig. 2A). The N content of the uncleaned samples was 103% higher than after the first oxidative cleaning (i.e. the control sample) for the North Atlantic mixed foraminifera sample, 250% higher for the Southern Ocean mixed foraminifera sample, 331% higher for the deep-sea coral, 46% higher for the shallow water coral, 309% higher for the modern elephant enamel sample, 305% higher for the fossil hippo enamel sample and 417% higher for the fossil suid enamel sample (Fig. 2C). The N content of the uncleaned diatom sample was only 7% higher than after the first oxidative cleaning, and not statistically significant. The large reduction observed in most fossil

354 types after the first cleaning was the expected result, because the purpose of this first cleaning
355 step was to remove external (non-mineral-bound) organic matter from the sample. The external
356 organic matter was likely mostly from the natural (e.g., sedimentary) environment in most cases,
357 but some of it may have derived from contamination during collection and storage.
358
359 Not surprisingly, the removal of the external organic N was associated with variable changes in
360 the isotopic composition of the different fossil types (Fig. 2B). The $\delta^{15}N$ of the North Atlantic
361 mixed foraminifera sample increased significantly by 1.25±0.16‰, but the $\delta^{15}N$ of the Southern
362 Ocean mixed foraminifera sample decreased significantly by 0.87±0.23‰ (Fig. 2D). The $\delta^{15}N$ of
363 the deep-sea coral increased significantly (by 0.67±0.11‰), while the shallow water coral $\delta^{15}N$
364 barely changed (decreasing by 0.06±0.19‰, but not significantly), despite the substantial
365 decrease in its N content. The $\delta^{15}N$ change of the diatom sample (from 0.93±1.21‰ to
366 1.78±0.02‰) was not significant, but cleaning resulted in a drastic decrease in standard
367 deviation. Suid and hippo fossil enamel showed large increases (2.99±0.40‰ and 4.21±1.30‰,
368 respectively), but modern enamel did not show a significant change (decreasing by
369 0.22±0.15‰), despite the large reduction in its N content. The absence of significant $\delta^{15}N$
370 changes in the modern enamel sample and the modern shallow-water coral core sample suggest
371 that most of the organic matter present in the drilled tooth enamel material and coral core was
372 endogenous to the organism and well-preserved despite not being bound to the mineral matrix.
373 However, the significant $\delta^{15}N$ change associated with the removal of external organic material in
374 other relatively recent (i.e. Holocene) samples (e.g. deep-sea coral and the two foraminifera
375 samples) and the very large change associated with the Plio-Pleistocene fossil enamel samples
376 highlight the potential for isotopically distinct N to become associated with fossil surfaces and
377 thus the need for harsh cleaning prior to the analysis of the N isotopic composition of fossil
378 bound organic material. Whether $\delta^{15}N$ increased or decreased upon cleaning could depend on
379 multiple factors, some of which may be identifiable. For example, foraminifera and diatoms
380 derive from deep sea sediments, and sedimentary organic N is known to undergo a diagenetic
381 increase in $\delta^{15}N$ (Freudenthal et al., 2001; Robinson et al., 2012), such that cleaning might be
382 expected to lower the $\delta^{15}N$ of the remaining N (i.e., the fossil-bound N). However, there are a
383 range of possible influences on the $\delta^{15}N$ of the external N, which vary with sample type and
384 sample origin. In addition, sample handling prior to analysis (e.g., drilling of coral and enamel

samples and washing, sieving and separation of foraminifera and diatom samples) can introduce N contamination. Thus, the reasons for the observed $\delta^{15}N$ changes upon cleaning (e.g., as to whether $\delta^{15}N$ increases or decreases) are not pursued further here.

Notably, the subsequent re-oxidation of all the samples analyzed resulted in negligible changes in N content and isotopic composition (Fig. 2A and 2B). In fact, for all fossil types analyzed, the N content and $\delta^{15}N$ of the re-oxidized samples were statistically indistinguishable from those obtained after a single oxidation (Fig. 2C and 2D). These results show that the mineral matrix indeed represents an effective physical barrier that protects organic matter against chemical attack, even with exceptionally strong oxidizing solutions (Fig. 6A).

Our findings are in good agreement with previous experiments designed to optimize the cleaning protocols of different fossil types (e.g., foraminifera, corals, tooth enamel, otoliths or diatoms) using either sodium hypochlorite or perchloric acid. In these experiments, the different fossil types were exposed to the oxidizing solutions for different times, either at room temperature, or with moderate heating to 60-70 ºC (Kast, 2020; Lueders-Dumont et al., 2018; Ren, 2010; Sigman et al., 1999). In general, all the studies showed a drop in N content and changes in $\delta^{15}N$ after a few hours of exposure to the reagent, as expected from the removal of the external (non-bound) organic matter. However, the N content and $\delta^{15}N$ of the sample stabilized with time, so that any additional time exposure to the reagent did not change N content or isotopic composition. In general, the application of heat resulted in a faster removal of the external organic matter, but did not change the N content or the $\delta^{15}N$ of the fossils analyzed with respect to that of the samples oxidized at room temperature. The original aim of these studies was to identify the optimal time and chemical reagent for the complete removal of external organic matter, but they also provided strong support for the stability of fossil-bound material.

In previous work, one exception to these uniformly straightforward findings has involved the cleaning of diatom frustules. Very fresh diatom opal, such as from diatom cultures, appears to be vulnerable to specific reagents, such as hydrogen peroxide (Morales et al., 2013). However, diatom opal is rapidly altered in the marine environment, for example, increasing its aluminum content by more than ten times upon incorporation in the sediments (Ren et al., 2013). This

alteration appears to "harden" the mineral to render it robust against hydrogen peroxide. Still, for Holocene opal oozes from the North Pacific, there are signs that diatom microfossils might not be able to protect fossil-native N against boiling perchloric acid (Brunelle et al., 2007). As described below, the heating experiments from the current study may explain these earlier results.

Previous work also suggests that, for diatom opal, some oxidative reagents and treatments can be too weak to fully remove externally vulnerable N, which required extensive testing to settle on the current cleaning protocol (Brunelle et al., 2007; Robinson et al., 2004). In contrast, for carbonate and phosphate biominerals, reagent choices (e.g., persulfate *vs.* hypochlorite) have shown little to no influence (Kast, 2020; Leichliter et al., 2021; Lueders-Dumont et al., 2018; Ren et al., 2009; Straub, 2012), albeit with a recrystallization-related exception for the otoliths of one fish species (Lueders-Dumont et al., 2018). We suspect that this difference of diatom opal from calcium carbonate and phosphate minerals relates to the unique and mutable characteristics of diatom opal, as will be discussed further in the context of the heating experiments in Section 3.3.

Our oxidant exposure experiments were, of course, not conducted on the geologic time scale, i.e., over thousands to millions of years. In this and other regards, the experiments are not an ideal simulation of the exposure of fossil material to sedimentary diagenesis. However, the oxidants used were far more aggressive than those used by microbes to attack sedimentary organic matter. Thus, our findings are strongly supportive of the view that fossil-bound N is well protected by the mineral matrix from the external environment, supporting the argument that fossil-bound N preserves the $\delta^{15}N$ of fossil-native organic matter generated by ancient organisms.

3.2 Impact of biomineral dissolution on foram-, coral-, tooth enamel- and diatom-bound $\delta^{15}N$

In our first set of experiments, samples were measured directly after the dissolution treatment (left panels in Fig. 3). The results of this first experiments showed a progressive increase in N content per mg of mineral as we increased the percentage of dissolved mineral matrix (Fig. 3A and 3C). The proportional N content increase found in the most aggressive treatment was similar

447 for foraminifera (20-34%) and corals (21-22%), slightly higher for tooth enamel (32-42%)
448 samples, and substantially lower for diatoms (2%) (Fig. 3C). The observed N content increase
449 from the most aggressive treatment was statistically significant compared to the untreated sample
450 for all the fossil types, except for the diatom sample.
451
452 The observed increase in N content during dissolution could indicate that: (i) organic matter
453 exposed during the dissolution experiment was not completely removed by rinsing multiple
454 times with Milli-Q water, or (ii) dissolution preferentially occurred in N-poor parts of the
455 mineral matrixes. In order to test these two hypotheses, we repeated the dissolution experiment,
456 but introducing a second oxidative cleaning step after the dissolution treatment (right panels in
457 Fig. 3). If the increase in N content was caused by incomplete removal of organic matter exposed
458 during dissolution, we would expect that this organic matter would be removed during this
459 additional oxidative cleaning. However, if it was caused by dissolution of N-poor regions of the
460 fossils, we would expect that the increasing N content trend would persist after the additional
461 cleaning. Our results show that after the second cleaning, for all of the fossils except for the
462 shallow water coral, the N content of the fossils analyzed after the different dissolution
463 treatments was statistically indistinguishable from the untreated control sample. These results
464 clearly indicate that the N increase observed in the first experiment for most of the fossil types
465 was due to incomplete removal of organic matter that was exposed during the dissolution
466 treatment; and, consequently, they confirm that the dissolution did not have a significant
467 preference for N-rich or N-poor biomineral.
468
469 In contrast, for the shallow water coral, there was a similar decrease (of 16-20%) during all
470 dissolution treatments relative to the undissolved sample. For this sample, an argument can be
471 made that the first dissolution (of ~25%) did access N-rich skeletal material. The decline in N
472 content was relatively constant with respect to the fraction dissolved, which may indicate the
473 dissolution of a discrete N-rich biomineral component, as opposed to dissolution being guided by
474 a continuous range in biomineral N content. Scleractinian coral skeleton is observed to contain
475 microcrystalline septa that are associated with the onset of calcification (the “rapid accretion
476 deposits”, also referred to as “centers of calcification”), representing ~5% of the skeleton
477 (Stolarski, 2003). Spatially-resolved measurements indicate that the rapid accretion deposits are

478 microcrystalline and richer in organics as well as non-calcium cations than the "thickening
479 deposits", the main skeletal component (Cuif and Dauphin, 2005). There is also evidence that the
480 rapid accretion deposits are the first component to undergo diagenesis and recrystallization
481 (Frankowiak et al., 2013). Thus, there are both conceptual and observational expectations that
482 this material would be particularly vulnerable to acid dissolution. Accordingly, the 16-20%
483 decline in N content of the coral sample under any level of acid addition in our experiments may
484 reflect the nearly complete dissolution of this microcrystalline component. However, the
485 observed changes in N content were relatively small, and deep-sea corals did not show a clear N
486 content decrease, especially in the 74% dissolution experiment. Thus, this hypothesis remains to
487 be confirmed by future experiments.
488
489 Despite the differences in N content found in most fossil types between our two versions of the
490 dissolution experiment (i.e., with and without subsequent oxidative cleaning), our results indicate
491 that the effect of partial dissolution on $\delta^{15}N$ was minimal in both cases (Fig. 3E to 3H). In most
492 of the fossils, the difference between the acid treatments and the untreated samples was within
493 0.4‰ (Fig. 3G and 3H), i.e., within 2 standard deviations of the average analytical precision
494 observed for the control standards (see Section 2.3).
495
496 We first consider the implications of the second experiment (with subsequent oxidative
497 cleaning), which is the better analogue for actual samples. In this experiment, the lack of change
498 in dissolved relative to undissolved samples indicates that the dissolution did not preferentially
499 remove isotopically distinct N (Fig. 6). This is not surprising. For isotopic change to have
500 occurred, there would need to be both (i) distinct solubilities among components of the
501 biomineral and (ii) isotopic differences that correlate with the susceptibility to dissolution. Our
502 results show very little change in N content, already arguing that N content variations, if they
503 occur at all, are not strongly correlated with biomineral variation. Otherwise, the comparison of
504 our two experiments confirm that any N exposed by the dissolution process is successfully
505 removed by our fossil cleaning.
506
507 Turning to the first experiment (i.e., without subsequent oxidative cleaning), beyond the
508 conclusions stated above, the N content increases indicate that a portion of the N exposed during

dissolution has an adequately robust structural (biochemical) framework to remain attached at the biomineral surface during repeated rinsing of the sample with Milli-Q water (Fig. 6). However, the $\delta^{15}N$ results indicate that this now-superficial N was not greatly changed in $\delta^{15}N$ by the dissolution process. This, again, is not surprising. Peptide bond hydrolysis could induce significant isotopic fractionation (Bada et al., 1989). However, protein hydrolysis requires much higher acid/base concentrations and temperatures, and longer reaction times (Roach and Gehrke, 1970). Accordingly, in our experiments, some N could be exhumed and survive the dissolution on the mineral surface, without undergoing clear isotopic changes in the process. Most of the data are consistent with this scenario.

We now turn to the few isotopic changes that were observed. In our first experiment (i.e., without subsequent oxidative cleaning), the biggest difference in $\delta^{15}N$ with respect to the untreated samples (-0.96±0.49‰) was observed after the 87% dissolution treatment of one of our fossil enamel samples (Fig. 3E and 3G). This treatment also resulted in one of the largest increases in N content (42%) with respect to the untreated sample. However, due to the relatively large standard deviation in $\delta^{15}N$ obtained for replicate analysis of the fossil, this difference was not statistically significant ($p = 0.03$). The large standard deviation obtained for the untreated sample, and across the different treatments, suggests a more heterogenous isotopic composition for this particular fossil. Interestingly, in the case of the modern enamel sample, dissolution treatments up to 91% resulted in negligible changes in $\delta^{15}N$ values ($p = 0.08$), despite the large increase in N content (32%) relative to the untreated sample. The diatom sample showed one of the lowest changes in $\delta^{15}N$ (0.15±0.03‰) during the most aggressive treatment (69% dissolution). Paradoxically, this difference was statistically significant with respect to the untreated sample due to the extremely low standard deviation of the diatom replicate measurements. The only other sample that showed a statistically significant difference (0.56±0.21‰) was the shallow water coral sample when dissolved by 47-70%. The differences observed in all the other coral, foraminifera and tooth fossils were statistically indistinguishable from the untreated samples.

In our second experiment (i.e., with subsequent oxidative cleaning), the difference between the different dissolution treatments and the untreated samples were even smaller (Fig. 3F and 3H). In

contrast to the first experiment, the shallow-water coral sample was undistinguishable from the control sample in all the treatments. However, the deep-water coral sample showed a statistically significant difference with respect to the untreated sample. Unfortunately, we could not perform the second experiment for the suid fossil enamel sample nor for the diatom sample because no sample powder was left. Nevertheless, the rest of the fossil samples analyzed, including an additional Plio-Pleistocene fossil enamel sample, were indistinguishable from the untreated samples (Fig. 3F and 3H). We consider this second experiment more directly comparable to environmental samples that were exposed to dissolution in the past, because any fossil-native organic matter that might have been exposed during dissolution would be removed by our standard cleaning protocol and not measured.

The fact that the $\delta^{15}N$ of the diatom exposed to ~70% dissolution and the deep-sea coral samples were statistically different from the untreated sample is not particularly concerning for the application of the fossil-bound $\delta^{15}N$ method. The diatom samples were isolated from deep-sea sediment cores. Thus, they have already undergone substantial dissolution in the water column and sediments as part of normal diagenetic processes (Van Cappellen et al., 2002). The ~70% further dissolution would thus represent an extreme degree of dissolution relative to the starting diatom opal material. Despite this situation, the observed $\delta^{15}N$ changes were very small (0.15±0.03‰) and would not significantly impact the palaeoceanographic interpretation. The deep-sea coral $\delta^{15}N$ increase (of 0.59±0.15‰) at 75% dissolution applied only to the dissolution experiment that included subsequent cleaning (Fig. 3H *vs*. 3G), which raises questions about its robustness. On the other hand, deep-sea corals record extensive periods of time and can capture major $\delta^{15}N$ changes (Wang et al., 2014), so the sample might be more heterogeneous and thus vulnerable to preferential loss of isotopically distinct material.

In summary, the stability of $\delta^{15}N$ after the different dissolution treatments indicate a generally uniform isotopic composition for foraminifera-, coral-, enamel-, and diatom-bound organic material, and imply that the N exposed during dissolution is lost without significant isotopic discrimination (Fig. 6). This conclusion is also supported by the similarity in the isotopic composition observed in our two experiments (with/without subsequent oxidative cleaning) despite significant differences in N content (Figs 3G and 3H). More practically, the second

experiment indicates that the partial dissolution of fossil opal, calcite, aragonite or enamel matrixes has a negligible effect on the N content and N isotopic composition of fossil-bound organic matter. These results are consistent with those obtained in a foraminifera $\delta^{15}N$ ground-truthing field study near Bermuda, which suggest that foraminifera-bound N loss during early seafloor diagenesis does not occur with significant isotope fractionation because any newly exposed N is completely lost rather than isotopically altered (Smart et al., 2018).

In addition, our dissolution experiment results provide a framework for understanding the effect of calcite recrystallization in marine sediments. A remarkable finding from the study of early Cenozoic planktonic foraminifera-bound $\delta^{15}N$ is that the fossil-bound N content and $\delta^{15}N$ are preserved (Kast et al., 2019) despite the evidence for substantial recrystallization and isotopic resetting of the foraminifer tests in deep sea sediments (Killingley, 1983; Pearson et al., 2001; Pearson et al., 2007). Our results indicate that the organic matter exposed by acid dissolution, at least in part, remains physicochemically connected with the surface of the remaining biomineral. Considering that the dissolution–reprecipitation of foraminiferal calcite is fast and occurs at a small spatial scale (Chanda et al., 2019), we hypothesize that the "exposed" organic N could be re-encapsulated in the recrystallized biomineral before it is lost or altered by bacterial attack.

3. 3 Impact of thermal decomposition on fossil-bound $\delta^{15}N$

As with the dissolution experiments, our first set of thermal degradation experiments samples were measured directly after the heating treatment, without a subsequent oxidative recleaning (left panels in Fig. 4). Our results showed no significant change in N content for all fossil types at 100 ºC and 200 ºC, except for diatoms (Figs. 4A and 4C). At temperatures > 200 ºC, deep and shallow water aragonitic coral samples showed a progressive decrease in N content of 12% and 42%, respectively, at 300 ºC, 49% and 59% at 400 ºC, and 80% and 79% at 500 ºC. In contrast, the two calcitic mixed foraminifera samples showed no significant N losses at 300 ºC, only a moderate decreased at 400 ºC (15% and 27%), and a large decline at 500 ºC (80% and 82%). Interestingly, at 400 ºC, the decline observed in the foraminifera was substantially smaller than the one found in the corals, but, at 500 ºC, N losses were comparable for both fossil types. Finally, the N content of the modern and fossil enamel samples was statistically indistinguishable from that of the untreated samples up to 400 ºC, and decreased by only 33% at 500 ºC in the

602 fossil sample, while there was not statistically significant N loss from the modern enamel
603 sample. Thus, tooth enamel is an interesting contrast with the ~80% reduction in calcitic
604 foraminifera and aragonitic corals. These results indicate that the fraction of N lost at different
605 temperatures depends on the mineral structure (and thus the mineral composition) of the fossil.
606
607 The effect of the different thermal treatments on the isotopic composition of fossil-bound N also
608 varied widely across the different fossil types analyzed (Fig. 4E and 4G). All fossils, except the
609 diatoms, showed negligible changes in $\delta^{15}N$ at 100 ºC. At 200 ºC, deep-sea corals increased with
610 respect to the untreated samples by 0.52±0.17‰, and the two foraminifera samples by
611 0.41±015‰ and 0.75±0.18‰, respectively, but the shallow water corals and the tooth enamel
612 samples showed no significant changes (Fig. 4G). At 300 ºC, deep-sea and shallow water coral
613 $\delta^{15}N$ increased moderately by 1.10±0.20‰ and 0.75±0.19‰, respectively. In contrast, the $\delta^{15}N$
614 increase observed in the two foraminifera samples (0.62±0.14‰ and 0.75±0.25‰) was
615 indistinguishable from the one observed at 200 ºC, while the two tooth enamel samples
616 continued to show no significant change. At 400 ºC, the $\delta^{15}N$ increase observed for the deep and
617 shallow corals (1.12±0.24‰ and 0.74±0.30‰), and the two foraminifera samples (0.67±0.16‰
618 and 0.95±0.16‰) was indistinguishable from that observed at 300 ºC. Again, the two tooth
619 enamel samples did not show any significant $\delta^{15}N$ change. Finally, at 500 ºC, the $\delta^{15}N$ increase
620 of the deep-sea coral (1.83±0.37‰) and the two foraminifera samples (3.19±0.32‰ and
621 3.57±0.49‰) was significantly higher than in the experiment performed at 400 ºC, and coincided
622 with substantial N loss, of about 80%. However, the $\delta^{15}N$ of the shallow water coral dropped to
623 values similar to those found in the untreated sample, despite a similar N loss. As in the previous
624 treatments, the two tooth enamel samples did not show any significant change at 500 ºC. Thus,
625 our results reveal that both the N loss and the degree of isotopic change at different temperatures
626 is directly linked to the mineral composition of the fossil.
627
628 In order to investigate further the relationship between N loss and $\delta^{15}N$ changes, we estimate the
629 isotope effect of thermal decomposition of fossil bound organic material. The isotope effect (ε)
630 expresses the degree of isotopic discrimination and is commonly defined as the ratio of reaction
631 rates at which the two isotopes are converted from reactant to product (i.e., ε (‰) = $((1- {}^{15}k/{}^{14}k) \times 1000)$; where ${}^{x}k$ is the rate constant for the ${}^{x}N$-containing reactant). We use the slope of the
632

633 correlation of $\delta^{15}N$ against the natural logarithm of the N content to obtain a Rayleigh model-
634 based estimate of the net isotope effect associated with the loss of N caused by thermal
635 decomposition of fossil bound organic material (upper panels in Fig. 5) (e.g. Fripiat et al. (2019).
636 If we plot our results across the entire temperature range, i.e. from room temperature (RT) to 500
637 ºC, we obtain a significant correlation for the two foraminifera samples and deep-sea coral, but
638 not for the shallow water coral and the tooth enamel samples (Fig 5A). However, the correlation
639 for the shallow water coral sample was significantly improved if the 500 ºC treatment was
640 excluded (Fig. 5B). From RT to 400 ºC, the correlation for the deep-sea coral sample was still
641 significant, but it was not for the foraminifera samples. From RT to 300 ºC, the correlation was
642 only significant for the shallow water coral sample. Interestingly, the estimated isotope effects
643 for the two coral samples were relatively similar (ranging from -0.80‰ to -1.04‰) from RT to
644 500 ºC and 400 ºC, suggesting that the isotopic discrimination during thermal degradation was
645 relatively similar at different temperatures for aragonitic samples. The isotope effects from the
646 two foraminifera samples were also very similar to one another (-1.76‰ and -1.22‰),
647 suggesting a slightly higher isotope effect for calcite than for aragonite. Finally, as expected from
648 the lack of variability in N content and $\delta^{15}N$, the correlation for the two tooth enamel samples
649 was not significant across any of the temperature ranges analyzed. Thus, our results raise the
650 possibility that the isotope effects during thermal degradation of fossil bound organic matter are
651 different for aragonite, calcite and apatite samples.
652
653 As an alternative possibility, there may be isotopically distinct forms of N that are preferentially
654 lost and retained that could explain or contribute to isotopic changes. In this case, the similar
655 isotope effects observed for different biominerals could relate more to the organisms producing
656 the fossil-bound N rather than the biomineral itself. Our strongest argument against this
657 alternative interpretation is that nearly all regressions yield a weak negative (or insignificant)
658 slope, which would seem unlikely if the isotopic changes were driven by preferential loss of
659 specific N forms in different types of organisms.
660
661 During this first set of experiment, the behavior of the diatom sample was not consistent with the
662 rest of the fossils and/or with expectations from thermal degradation of frustule bound organic
663 matter. Our results showed substantial increases in N content (~300%) with respect to the

664 untreated sample at 100 ºC, suggesting substantial contamination of the frustule material with
665 exogenous N (Fig. 4A and 4C). This N content increase was accompanied by a significant
666 reduction in $\delta^{15}N$ values (of 2.56‰) (Fig. 4E and 4G). This contamination problem persisted at
667 higher temperatures, and the N content of the treated samples at 200 ºC and 300 ºC was still
668 higher (and the $\delta^{15}N$ significantly lower) than that of the untreated control sample. A mass
669 balance of the N change between the control sample and the 100 ºC measurements reveals that
670 the $\delta^{15}N$ of the N added was 0.28‰. The ability of diatom opal to adsorb N species has been
671 noted previously (Robinson et al., 2004), and it also appears to apply to carbon species (Zheng et
672 al., 2002). We have not as yet investigated further the mechanism or form of the opal N
673 contamination. However, we suspect that it derives from some of the same characteristics of
674 diatom opal that also lead to the unique sensitivity of diatom-bound $\delta^{15}N$ to the cleaning
675 protocol, as discussed in section 3.1. The high effective surface area of opal and its potential for
676 chemical and structural transformation upon heating (e.g, associated with opal dehydration) may
677 allow for the exposure, alteration, and release of diatom-native N, as well as uptake of exogenous
678 N species, close to the opal surface. In any case, these results indicate that heated diatom opal
679 requires recleaning to remove adsorbed N.
680
681 As with our investigation of partial dissolution, we performed a second set of heating
682 experiments in which an oxidative recleaning step was added after the heating treatment (right
683 panels in Fig. 4). This second experiment allowed us to further investigate: (i) the effect of N
684 absorption into the opal, and (ii) to what extent the observed changes in $\delta^{15}N$ in the different
685 treatments involved the organic matter that remained bound within the mineral or only organic
686 matter that could have been exposed during heating. As in the case of the dissolution
687 experiments, any adsorbed or exposed organic material would be removed during the second
688 oxidative cleaning, allowing us to analyze only the fraction of organic material that remained
689 protected within the biomineral matrix. An additional motivation for this suite of experiments is
690 that they better address the situation of fossil-bound N isotopic analysis of naturally heated
691 samples because fossil samples are always cleaned before they are measured.
692
693 In this second set of experiments, the observed N content trends were, in general, very similar to
694 those obtained in our first set of experiments for all fossil types, except for the diatoms (Fig. 4B

695 and 4D). These findings indicate that the additional cleaning step did not remove a substantial
696 amount of organic matter that was exposed during heating but that remained on the surface of the
697 fossil material. This indicates that the organic matter exposed by heating is subsequently almost
698 completely lost from the fossil material. This is not surprising because, at temperatures > 300 ºC,
699 we would expect that the exposed organic material would be combusted and thus volatilized into
700 the air.
701
702 Nevertheless, we observe a few small, but in some cases significant, differences in the $\delta^{15}N$
703 trends of some fossils between the "un-recleaned" and "recleaned" heating experiments. These
704 differences suggest that some small amount of organic matter was exposed and altered during
705 heating and was subsequently removed during the recleaning (Fig. 6C). The removed N was
706 probably too small to be detected in our N content measurements, but its isotopic composition
707 may have been different enough to slightly change the $\delta^{15}N$ of the fossils in some cases. In
708 particular, in the recleaned experiment, the $\delta^{15}N$ of the two foraminifera samples was
709 indistinguishable from the reference in the range from 100 ºC to 400 ºC, and it was only
710 statistically different at 500 ºC, indicating that foraminifera calcite was stable up to 400 ºC. The
711 two coral samples showed similar trends as in the un-recleaned experiment, but the difference
712 with respect to the reference sample was smaller, particularly for the deep-sea coral. As in the
713 un-recleaned experiments, the modern and fossil enamel samples showed no significant change
714 in the range of temperatures analyzed, but the fossil enamel showed larger increases at 400 ºC
715 (0.91±0.35‰), and 500 ºC (0.73±0.31‰), suggesting that it may be less robust than modern
716 enamel when exposed to very high temperatures. Regarding the calculated isotope effects (Fig.
717 5), overall, they were somewhat smaller than those obtained in the un-recleaned experiment,
718 suggesting that the values obtained in the un-recleaned experiments may slightly overestimate
719 the fractionation induced by thermal removal of fossil-bound N. This may be due to more intense
720 isotopic alteration of organic N that is exposed but not removed during the heating treatment. It
721 is worth noting that the isotope effects obtained for foraminifera and corals were very low
722 (typically < 1‰), indicating that the potential biases introduced by thermal alteration would be
723 small even if they result in significant N loss (> 90%), as observed at 500 ºC.
724

In contrast to the similar trends observed for rest of the fossils in both sets of experiments, the diatom samples showed a very different pattern upon recleaning after the heating treatment. The measurements of the recleaned diatom samples suggest that the recleaning did effectively remove the adsorbed N that contaminated the samples in the first experiment. In the recleaned heating experiment, diatoms showed no significant change in N content or $\delta^{15}N$ at 100 ºC (Fig. 4D and 4H). At 200 ºC, they indicated a small but statistically significant reduction in N content (15%), accompanied by a 0.92±0.04‰ increase in $\delta^{15}N$. At temperatures > 200 ºC, the diatom sample showed the greatest decrease in N content of all the fossil types analyzed, with declines of 58% at 300 ºC, 94% at 400 ºC, and 99% at 500 ºC. This sharp decrease in N content was accompanied by large changes in $\delta^{15}N$. At 300 ºC, diatom $\delta^{15}N$ increased with respect to the untreated control sample by 4.44±0.06‰, and at 400 ºC, it increased by 5.46±0.15‰. In contrast, at 500 ºC, diatoms showed a somewhat smaller increase in $\delta^{15}N$ than at 400 ºC and 300 ºC, despite of the 99% decrease in its N content. Consistent with these observations, the calculated isotope effect for the diatom sample N loss varied substantially, ranging from -5.33‰ between the control sample and 300 ºC to -0.99‰ between the control and 500 ºC (Fig. 5D to 5F). These results may suggest the removal of different types of frustule-bound organic matter at different temperatures, with different isotopic compositions and/or different isotope effects applying to each type. However, the nearly complete loss of the initial diatom-bound N at the highest temperatures argues for caution in interpreting these results. In any case, our results suggest that the diatom-bound $\delta^{15}N$ of environmental samples exposed to temperatures above 100 ºC, and especially above 200 ºC, would likely be altered.

Overall, the patterns observed for the different fossil types indicate that both the N loss and the degree of isotopic change at different temperatures are directly linked to the robustness of the mineralogy and structure of the fossil. Thermogravimetric analysis of pretreated *Pinnularia* diatom frustules has shown that substantial sample weight loss associated with the removal of the organic fraction of the frustule starts to occur at temperatures between 200 ºC and 300 ºC, and continues until 550 ºC, above which no further decrease in weight is detected (Van Eynde et al., 2014). Biogenic aragonite (from powdered *Acropora* corals) starts to transform to calcite at 280 ºC and is completely transformed to calcite at 380 ºC (Yoshioka and Kitano, 1985). Substantial calcite decomposition typically begins between 500 ºC and 550 ºC, although marine carbonates

may already become unstable at temperatures between 400 ºC and 500 ºC due to the presence of magnesium (Hirota and Szyper, 1975). Tooth enamel suffers structural and chemical alteration in response to thermal stress mainly at temperatures above 600 ºC (Robinson and Kingston, 2020; Shipman et al., 1984).

These ranges of decomposition temperatures for opal, aragonite, calcite and enamel are consistent with the temperatures at which we start to observe substantial N loss and $\delta^{15}N$ changes in diatoms, corals, foraminifera and tooth enamel samples. The observation of significant N content and $\delta^{15}N$ changes in diatoms at 200 ºC and the large degrees of N loss indicate that the frustule material becomes permeable to N at high temperatures. The N loss and associated $\delta^{15}N$ change observed in coral samples at 300 ºC was likely associated with the conversion of aragonite to calcite. However, the smaller proportional change in N content observed between 300 ºC and 400 ºC suggests that part of the coral-bound N was still trapped in the newly forming calcite. The subsequent N loss and $\delta^{15}N$ change observed at 500 ºC was consistent with the one observed in the calcitic foraminifera samples, and it was likely associated with the decomposition of calcite in both cases. Finally, the absence of significant changes in N content and isotopic composition of modern enamel up to 500 ºC is consistent with minor alteration of the matrix at this temperature. However, the changes observed in fossil tooth enamel at 400 ºC and 500 ºC suggest that aging may cause enamel to become less robust to thermal stress, at least at these extreme temperatures.

Our results, when compared to these temperatures for biomineral modification, suggest that the mineral matrix of the fossil acts as a nearly closed system with respect to N, up to the point that heating compromises the integrity of the mineral matrix itself (Fig. 6C). A previous study has shown that in *Porites* coral powder heated under aqueous conditions at 80 ºC, 110 ºC and 140 ºC, the amino acid concentrations in the supernatant water remained within the analytical limit of detection despite of substantial changes in the chemical composition of intra-crystalline amino acids, indicating that the carbonate skeleton retained this organic N pool (Tomiak et al., 2013). Our new experiments are consistent with these observations and indicate that not only amino acids but also total N is retained within the mineral matrix at temperatures of 100 ºC in all the fossil types analyzed. Hence, our results indicate a negligible effect of thermal degradation on

fossil-bound organic matter N isotopic composition in the range of temperatures associated with local geothermal gradients in Cenozoic marine sediments, which are typically less than 60 ºC (Malinverno and Martinez, 2015). In addition, our data reveal that, in some cases (e.g., calcite or enamel), N can remain isotopically unaltered within the mineral matrix even at temperatures well above the typical combustion temperatures of protein amino acids, which range from 185 ºC to 280 ºC (Weiss et al., 2018). These findings suggest that the fossil-bound N isotope method could be applied in enamel, calcitic and even aragonitic fossil samples that have suffered substantial thermal stress without significant biases in the measured $\delta^{15}N$ values. However, further work is required to fully explore this possibility.

In contrast, our experiments suggest that diatom deposits exposed to temperatures above 100 ºC, and especially above 200 ºC, would experience substantial diatom-bound organic matter degradation that could significantly bias the N isotopic signal. Our observations may also help to explain some previous observations regarding the sensitivity of diatom-bound $\delta^{15}N$ to the cleaning protocol used. It has been noted that diatom opal from particularly opal-rich sediments, which tends to have a lower Al/Si ratio (Ren et al., 2013), has diatom-bound N that is vulnerable to $\delta^{15}N$ alteration by boiling in perchloric acid (Brunelle et al., 2007; Robinson et al., 2004). Moreover, this effect appears to be absent in diatom opal from glacial-age samples, in which the opal has a higher Al/Si ratio (Brunelle et al., 2007; Ren et al., 2013). The temperature of boiling perchloric acid is greater than 100 °C, increasing with dehydration. Our temperature treatment experiments indicate that diatom frustules can both lose and gain N, due to thermal modification of the diatom opal above 100 ºC. Thus, the previous findings regarding diatom cleaning may be explained by the effect of treatment temperature on the structural integrity of the diatom opal.

4 Conclusions

Our experiments performed under controlled laboratory conditions indicate the following.

(i) Fossil-bound organic matter is effectively isolated by the mineral matrix from chemical changes in the surrounding environment.

817 (ii) Fossil-bound organic matter is removed without isotopic discrimination by partial
818 dissolution of the mineral matrix.
819 (iii) In the fossil types investigated, fossil-bound organic matter has a relatively uniform N
820 isotopic composition across the mineral matrix.
821 (iv) The fossil-native organic matter exposed by acid dissolution remains, at least in part, as a
822 physicochemical framework connected with the remaining biomineral. If recrystallization
823 occurs at a scale that minimizes exposure of this organic N to microbes, our observations offer
824 a possible explanation for the apparent stability of fossil-bound organic matter in
825 recrystallized biominerals (e.g., (Kast et al., 2019).
826 (v) During heating, the mineral matrix behaves as a nearly closed system with respect to N, up
827 to the point that the high temperature compromises the integrity of the mineral matrix itself.
828
829 Thus, our results provide strong experimental support for the robustness of fossil-bound organic
830 matter to reconstruct the original N isotopic composition of ancient organisms. We acknowledge
831 that the full range of diagenetic reactions found in the environment on geological timescales are
832 difficult to simulate in the laboratory. Thus, direct observations from the geologic past are also
833 necessary to provide a more complete assessment of the potential diagenetic effects on fossil-
834 bound organic matter. In this vein, the results obtained here are consistent with observations
835 from the geologic past. First, a number of studies have shown that the N content of fossils of the
836 same species/genus remains relatively stable across thousands to millions of years, suggesting
837 that mineral matrix acted as a closed system with respect to N (Auderset et al., in press; Kast et
838 al., 2019; Leichliter et al., 2021; Ren et al., 2017; Studer et al., 2012). This observation is
839 consistent with our findings indicating a similar behavior for fossil and modern enamel across
840 the different experiments, suggesting that aging may not affect substantially the robustness of the
841 mineral matrix, except perhaps at extreme temperatures (i.e., above 400 ºC). Second, different
842 species of foraminifera, which have different sensitivities to alteration of the mineral matrix,
843 reveal consistent $\delta^{15}N$ changes (Ren et al., 2017; Ren et al., 2015; Straub et al., 2013). Third,
844 foraminifera, corals and diatoms, which have different sensitivities to alteration, provide
845 consistent estimates of regional $\delta^{15}N$ changes when measured across the same time periods and
846 in the same regions (Ai et al., 2020; Martinez-Garcia et al., 2014; Studer et al., 2015; Wang et
847 al., 2017).

The evidence, reported here and previously, for the robustness of fossil-bound N has implications from prior comparisons of fossil-bound and bulk sediment $\delta^{15}N$, which often shows dramatic differences (Martinez-Garcia et al., 2014; Ren et al., 2017; Robinson et al., 2005; Straub et al., 2013; Studer et al., 2021). Bulk sediment $\delta^{15}N$ is known to be sensitive to diagenetic alteration and contamination by terrestrial N inputs (Robinson et al., 2012). In contrast, so long as the diagenetic conditions are appropriate to preserve the biomineral in question, fossil-bound $\delta^{15}N$ appears to be remarkably robust. Even in situations of biomineral dissolution/recrystallization, such as in early Cenozoic, carbonate-rich deep-sea sediments, N content and $\delta^{15}N$ data indicate the preservation of fossil-bound N (Kast et al., 2019), which is consistent with the results of the dissolution experiments presented here. Thus, the comparison of fossil-bound and bulk sediment $\delta^{15}N$ could offer insights into diagenetic processes affecting sedimentary organic matter (Martinez-Garcia et al., 2014), or into changes in terrestrial N inputs (Ren et al., 2017; Ren et al., 2009; Straub et al., 2013). Alternatively, if one seeks to argue that the fossil-bound N is "to blame" for a disagreement with bulk sediment $\delta^{15}N$, or if differences in fossil-bound-$\delta^{15}N$ are found among different fossil types or species, one must look to the biological controls on the isotopic signatures incorporated into fossil-bound organic matter by the fossil-producing organisms. This situation motivates an expansion of ground-truthing research that focuses on the biological and ecological controls on the N encapsulated within different types of newly generated biominerals.

Acknowledgements

This study was funded by the Max Planck Society. T.L. acknowledges funding from Emmy Noether Fellowship (LU 2199/2-1), and D.M.S. acknowledges funding from the U.S. National Science Foundation (PLR-1401489, OCE-2054780). The authors thank Barbara Hinnenberg and Florian Rubach for technical support during sample analysis and preparation of standard materials.

Author contribution

A.M-G designed the experiments, supervised the analysis of the samples and wrote the manuscript, with feedback from D.M.S. J.J. performed the experiments on, and measured the

isotopic composition of the coral, foraminifera and tooth enamel standards. X.E.A. performed the experiments on, and measured the isotopic composition of the diatom standard. N.D. and A.F. prepared the coral standards and were involved in the analytical training of J.J. T.W. was involved in the characterization of the coral standards. A.A. prepared the foraminifera standards. F.F., S.M. and X.E.A. prepared the diatom standards. J.L. and T.L. prepared the tooth enamel standards. All authors were involved in the discussion of the data at different stages of the project and contributed to the final version of the manuscript.

Open Research

Data Availability Statement

All the data generated in this study are available in the Supporting Information.

Figure Captions:

Figure 1. Experimental Design. For each sample type, an aliquot of uncleaned powder was taken and used in our chemical oxidation experiment. The remaining powder was subsequently cleaned in four aliquots (of 50 mg each) following the reductive-oxidative cleaning methods described in Section 2.3. After cleaning, the dry fossil powder was combined in a single vial and homogenized. This homogenous cleaned powder was measured (at least in triplicate) and used as a control sample for all of our treatments. In our oxidation experiment, the uncleaned sample aliquot was measured in triplicate and compared to our control sample, and to an aliquot of the control sample that was oxidatively recleaned in triplicate. In our dissolution experiments, we performed three triplicate treatments in which approximately 25%, 50% and 75% of the control sample was dissolved. In our first dissolution experiment, the sample powders remaining after dissolution were rinsed five times with Milli-Q water and measured. In our second experiment, the powders were recleaned oxidatively before the measurement. In our heating experiments, the control sample powder was heated to 100 ºC, 200 ºC, 300 ºC, 400 ºC and 500 ºC. In our first experiment, samples were measured directly after heating; in our second experiment, samples were recleaned oxidatively before the measurement.

Figure 2. Evaluation of the effect of exposure to strongly oxidative conditions on fossil-bound $\delta^{15}N$. Effect of consecutive oxidative cleanings with solutions of bleach (corals), potassium peroxydisulphate (foraminifera and teeth) and perchloric acid (diatoms) on fossil-bound (A) N content and (B) $\delta^{15}N$. In (A), a $\log_{10}$ scale is used in the Y axis to facilitate comparison of the different fossil types. (C) Percent N content difference of 0 oxidations and 2 oxidations with respect to the 1 oxidation treatment. (D) Same difference as in (C) but for $\delta^{15}N$ instead of percent N content. The grey shaded area highlights differences between the treated and untreated samples that are within 0.4‰, i.e., within 2 standard deviations of the average analytical precision observed for the control samples (see Section 2.3). In (A) and (B) error bars represent the 1 sigma standard deviation of triplicate oxidation experiments performed for each treatment (see Fig. 1). In C and D error bars indicate the propagated uncertainty from A and B, respectively. Note that the untreated reference sample in this experiment is the sample that has been cleaned once, and not the uncleaned sample.

Figure 3. Evaluation of the effect of biomineral dissolution on fossil-bound $\delta^{15}N$. Left panels (A, C, E, G) show results for samples measured directly after the dissolution treatment. Right panels (B, D, F, and H) show results for samples that were subjected to an additional oxidative cleaning after the dissolution treatment. (A, B) N content and (E, F) $\delta^{15}N$ of different fossil types. In (A and B), a $\log_{10}$ scale is used in the Y axis to facilitate comparison of the different fossil types. (C, D) Percent N content difference between each dissolution treatment and the untreated sample. (G, H) $\delta^{15}N$ difference between each dissolution treatment and the untreated sample. The grey shaded area highlights differences between the treated and untreated samples that are within 0.4‰, i.e., within 2 standard deviations of the average analytical precision observed for the control samples (see Section 2.3). In A, B, E and F, error bars represent the 1 sigma standard deviation of triplicate dissolution experiments performed for each treatment (see

Fig. 1). In C, D, G, and H, error bars indicate the propagated uncertainty from A, B, E and F, respectively.

Figure 4. Evaluation of the effect of heating on fossil-bound $\delta^{15}N$. Left panels (A, C, E, G) show results for samples measured directly after the heating treatment. Right panels (B, D, F, and H) show results for samples that were subjected to an additional oxidative cleaning after the heating treatment. (A, B) N content and (E, F) $\delta^{15}N$ of different fossil types. Notice that in (A and B) a $\log_{10}$ scale is used in the Y axis to facilitate comparison of the different fossil types. (C, D) Percent N content difference between each heating treatment and the control sample, i.e. room temperature (RT). In C, percent N content values for the DI-2 sample are plotted in the right axis. (G, H) $\delta^{15}N$ difference between each heating treatment and the control sample. The grey shaded area highlights differences between the treated and untreated samples that are within 0.4‰, i.e., within 2 standard deviations of the average analytical precision observed for the control samples (see Section 2.3). In A, B, E and F, error bars represent the 1 sigma standard deviation of triplicate heating experiments performed for each treatment (see Fig. 1). In C, D, G, and H, error bars indicate the propagated uncertainty from A, B, E and F, respectively.

Figure 5. Evaluation of the isotope effect associated with thermal degradation of fossil-bound $\delta^{15}N$. Upper panels (A, B, C) show results for samples measured directly after the heating treatment. Lower panels (D, E, F) show results for samples that were subjected to an additional oxidative cleaning after the heating treatment. The figure shows fossil-bound $\delta^{15}N$ *vs.* the natural logarithm (ln) of the N content for the different temperature treatments shown in Fig 4. (A) Considering data from the entire temperature range from room temperature (RT), i.e. our control sample, to 500 ºC, (B) from RT to 400 ºC, and (C) from RT to 300 ºC. The slope of the linear regressions (indicated above each plot) provides an estimate of the isotope effect (ε) associated with the loss of N from the fossil (see text). Error bars represent the 1 sigma standard deviation of triplicate experiments performed for each treatment.

Figure 6. Summary of the interpretation of the oxidation, dissolution and heating experiments. (A) In our oxidation experiments, our reductive + oxidative cleaning causes a substantial reduction in N content and a change in $\delta^{15}N$ that is consistent for a given standard but varies among different standards and fossil types (Fig. 2C and 2D). We interpret these changes to reflect the removal of external OM (red lines). However, the oxidative recleaning did not produce any significant changes in N content or $\delta^{15}N$, indicating that FB-OM (green lines) was effectively protected from chemical attack by the biomineral. (B) Our dissolution experiments reveal a progressive increase in N content per mg of calcite as dissolution increased (Fig. 3C). This change in N content occurred without substantial change in $\delta^{15}N$ (Fig. 3G). The progressive increase in N disappeared after an additional oxidative cleaning (Fig. 3D), without substantial change in $\delta^{15}N$ (Fig. 3H). These results indicate that part of the FB-OM was exposed after dissolution, but it was not altered, and remained physiochemically attached to the biomineral (exposed green lines). This OM was not removed during rinsing with Milli-Q water, but it was completely eliminated with an oxidative recleaning. The stability of the $\delta^{15}N$ values obtained before and after the recleaning demonstrate that FB-OM has a relatively homogenous isotopic composition, and that it was not altered during the dissolution process. (C) Our results indicate

no significant changes in FB N content or $\delta^{15}N$ at temperatures ≤ 200 ºC in any of the corals, foraminifera or teeth analyzed, regardless of whether samples underwent oxidative recleaning (Fig. 4C, 4D, 4G, and 4H). These results indicate that, despite potential changes in the molecular structure of the FB-OM (dashed green lines) that could be induced by heating (Tomiak et al., 2013), the biomineral acted as a closed system with respect to N. Corals showed substantial N content changes at temperatures ≥ 300 ºC, foraminifera and fossil enamel at ≥ 400 ºC, while modern enamel remained stable even at 500 ºC (Fig. 4C and D). Despite these substantial changes in N content, after oxidative recleaning, the $\delta^{15}N$ of corals, foraminifera and fossil teeth showed minimal changes (Fig. 4H). This suggests that the proportion of altered FB-OM that remained in the samples (pink lines) was very small. Diatoms show a very different response to heating than the rest of the fossils. When they were not oxidatively recleaned after heating, N content increased and $\delta^{15}N$ decreased significantly (Fig. 4C and 4G), suggesting contamination of the samples by adsorption of N during heating. This contamination was successfully removed by recleaning (Fig. 4D). In contrast to the other fossil types, in diatoms, substantial N loss was observed even at temperatures ≥ 200 ºC, and it was associated with substantial $\delta^{15}N$ changes (Fig. 4C and 4G). These findings suggest the presence of a larger proportion of altered FB-OM (pink lines) in diatoms than in other fossil after heating. Overall, our results indicate that N loss depends on the resistance of the biomineral itself to thermal stress. The potential alteration of FB-OM was significant for diatoms at temperatures ≥ 200 ºC, but higher temperature thresholds were observed for corals, foraminifera and tooth enamel.

References:

Ai, X.E., Studer, A.S., Sigman, D.M., Martínez-García, A., Fripiat, F., Thöle, L.M.*, et al.* (2020) Southern Ocean upwelling, Earth's obliquity, and glacial-interglacial atmospheric CO_2 change. *Science* 370, 1348-1352. doi:10.1126/science.abd2115

Altabet, M.A. and Curry, W.B. (1989) Testing models of past ocean chemistry using foraminifera $^{15}N/^{14}N$. *Global Biogeochemical Cycles* 3, 107-119. doi:10.1029/GB003i002p00107

Arndt, S., Jørgensen, B.B., LaRowe, D.E., Middelburg, J.J., Pancost, R.D. and Regnier, P. (2013) Quantifying the degradation of organic matter in marine sediments: A review and synthesis. *Earth-Science Reviews* 123, 53-86. doi:10.1016/j.earscirev.2013.02.008

Auderset, A., Moretti, S., Taphorn, B., Ebner, P., Kast, E.R., Wang, X.T.*, et al.* (in press) Enhanced ocean oxygenation during Cenozoic warm periods. *Nature*.

Bada, J.L., Schoeninger, M.J. and Schimmelmann, A. (1989) Isotopic fractionation during peptide bond hydrolysis. *Geochim. Cosmochim. Acta* 53, 3337-3341. doi:10.1016/0016-7037(89)90114-2

Bai, Y., Yu, Z., Ackerman, L., Zhang, Y., Bonde, J., Li, W.*, et al.* (2020) Protein nanoribbons template enamel mineralization. *Proceedings of the National Academy of Sciences* 117, 19201-19208. doi:10.1073/pnas.2007838117

Braman, R.S. and Hendrix, S.A. (2002) Nanogram nitrite and nitrate determination in environmental and biological materials by vanadium(III) reduction with chemiluminescence detection. *Analytical Chemistry* 61, 2715-2718. doi:10.1021/ac00199a007

Bridoux, M.C., Annenkov, V.V., Keil, R.G. and Ingalls, A.E. (2012a) Widespread distribution and molecular diversity of diatom frustule bound aliphatic long chain polyamines (LCPAs) in marine sediments. *Organic Geochemistry* 48, 9-20. doi:10.1016/j.orggeochem.2012.04.002

Bridoux, M.C., Keil, R.G. and Ingalls, A.E. (2012b) Analysis of natural diatom communities reveals novel insights into the diversity of long chain polyamine (LCPA) structures involved in silica precipitation. *Organic Geochemistry* 47, 9-21. doi:10.1016/j.orggeochem.2012.02.010

Brown, S.J. and Elderfield, H. (1996) Variations in Mg/Ca and Sr/Ca ratios of planktonic foraminifera caused by postdepositional dissolution: Evidence of shallow Mg-dependent dissolution. *Paleoceanography* 11, 543-551. doi:10.1029/96pa01491

Brunelle, B.G., Sigman, D.M., Cook, M.S., Keigwin, L.D., Haug, G.H., Plessen, B.*, et al.* (2007) Evidence from diatom-bound nitrogen isotopes for subarctic Pacific stratification during the last ice age and a link to North Pacific denitrification changes. *Paleoceanography* 22. doi:10.1029/2005pa001205

Burdige, D.J. (2006) Geochemistry of Marine Sediments. Princeton University Press.

Cappellini, E., Welker, F., Pandolfi, L., Ramos-Madrigal, J., Samodova, D., Rüther, P.L.*, et al.* (2019) Early Pleistocene enamel proteome from Dmanisi resolves Stephanorhinus phylogeny. *Nature* 574, 103-107. doi:10.1038/s41586-019-1555-y

Casciotti, K.L. (2016) Nitrogen and Oxygen Isotopic Studies of the Marine Nitrogen Cycle. *Annu Rev Mar Sci* 8, 379-407. doi:10.1146/annurev-marine-010213-135052

Castiblanco, G.A., Rutishauser, D., Ilag, L.L., Martignon, S., Castellanos, J.E. and Mejía, W. (2015) Identification of proteins from human permanent erupted enamel. *European Journal of Oral Sciences* 123, 390-395. doi:10.1111/eos.12214

1051 Chanda, P., Gorski, C.A., Oakes, R.L. and Fantle, M.S. (2019) Low temperature stable mineral
1052 recrystallization of foraminiferal tests and implications for the fidelity of geochemical proxies.
1053 *Earth Planet. Sci. Lett.* 506, 428-440. doi:10.1016/j.epsl.2018.11.011
1054 Cowie, G.L. and Hedges, J.I. (1994) Biochemical indicators of diagenetic alteration in natural
1055 organic matter mixtures. *Nature* 369, 304-307. doi:10.1038/369304a0
1056 Cuif, J.-P. and Dauphin, Y. (2005) The two-step mode of growth in the scleractinian coral
1057 skeletons from the micrometre to the overall scale. *Journal of Structural Biology* 150, 319-
1058 331. doi:10.1016/j.jsb.2005.03.004
1059 Cusack, M. and Freer, A. (2008) Biomineralization: Elemental and Organic Influence in
1060 Carbonate Systems. *Chem Rev* 108, 4433-4454. doi:10.1021/cr078270o
1061 Dauwe, B. and Middelburg, J.J. (1998) Amino acids and hexosamines as indicators of organic
1062 matter degradation state in North Sea sediments. *Limnology and Oceanography* 43, 782-798.
1063 doi:10.4319/lo.1998.43.5.0782
1064 Deniro, M.J. and Epstein, S. (1981) Influence of Diet on the Distribution of Nitrogen Isotopes in
1065 Animals. *Geochim. Cosmochim. Acta* 45, 341-351. doi:Doi 10.1016/0016-7037(81)90244-1
1066 Duprey, N.N., Wang, X.T., Kim, T., Cybulski, J.D., Vonhof, H.B., Crutzen, P.J.*, et al.* (2020)
1067 Megacity development and the demise of coastal coral communities: evidence from coral
1068 skeleton $\delta^{15}N$ records in the Pearl River estuary. *Global Change Biology*.
1069 doi:10.1111/gcb.14923
1070 Engel, M.H., Goodfriend, G.A., Qian, Y.R. and Macko, S.A. (1994) Indigeneity of Organic-
1071 Matter in Fossils - a Test Using Stable-Isotope Analysis of Amino-Acid Enantiomers in
1072 Quaternary Mollusk Shells. *Proceedings of the National Academy of Sciences of the United*
1073 *States of America* 91, 10475-10478. doi:DOI 10.1073/pnas.91.22.10475
1074 Engel, M.H. and Macko, S.A. (1986) Stable Isotope Evaluation of the Origins of Amino-Acids in
1075 Fossils. *Nature* 323, 531-533. doi:DOI 10.1038/323531a0
1076 Erler, D.V., Farid, H.T., Glaze, T.D., Carlson-Perret, N.L. and Lough, J.M. (2020) Coral
1077 skeletons reveal the history of nitrogen cycling in the coastal Great Barrier Reef. *Nat Commun*
1078 11. doi:10.1038/s41467-020-15278-w
1079 Erler, D.V., Wang, X.C.T., Sigman, D.M., Scheffers, S.R., Martinez-Garcia, A. and Haug, G.H.
1080 (2016) Nitrogen isotopic composition of organic matter from a 168 year-old coral skeleton:
1081 Implications for coastal nutrient cycling in the Great Barrier Reef Lagoon. *Earth Planet. Sci.*
1082 *Lett.* 434, 161-170. doi:10.1016/j.epsl.2015.11.023
1083 Farmer, J.R., Sigman, D.M., Granger, J., Underwood, O.M., Fripiat, F., Cronin, T.M.*, et al.*
1084 (2021) Arctic Ocean stratification set by sea level and freshwater inputs since the last ice age.
1085 *Nat Geosci* 14, 684-689. doi:10.1038/s41561-021-00789-y
1086 Frankowiak, K., Mazur, M., Gothmann, A.M. and Stolarski, J. (2013) Diagenetic Alteration of
1087 Triassic Coral from the Aragonite Konservat-Lagerstatte in Alakir Cay, Turkey: Implications
1088 for Geochemical Measurements. *Palaios* 28, 333-342. doi:10.2110/palo.2012.p12-116r
1089 Freudenthal, T., Wagner, T., Wenzhöfer, F., Zabel, M. and Wefer, G. (2001) Early diagenesis of
1090 organic matter from sediments of the eastern subtropical Atlantic: evidence from stable
1091 nitrogen and carbon isotopes. *Geochim. Cosmochim. Acta* 65, 1795-1808. doi:10.1016/s0016-
1092 7037(01)00554-3
1093 Fripiat, F., Martínez-García, A., Fawcett, S.E., Kemeny, P.C., Studer, A.S., Smart, S.M.*, et al.*
1094 (2019) The isotope effect of nitrate assimilation in the Antarctic Zone: Improved estimates
1095 and paleoceanographic implications. *Geochim. Cosmochim. Acta* 247, 261-279.
1096 doi:10.1016/j.gca.2018.12.003

1097 Fripiat, F., Martínez-García, A., Marconi, D., Fawcett, S.E., Kopf, S.H., Luu, V.H., *et al.* (2021)
1098 Nitrogen isotopic constraints on nutrient transport to the upper ocean. *Nat Geosci*.
1099 doi:10.1038/s41561-021-00836-8
1100 Gehler, A., Tutken, T. and Pack, A. (2012) Oxygen and carbon isotope variations in a modern
1101 rodent community - implications for palaeoenvironmental reconstructions. *Plos One* 7,
1102 e49531. doi:10.1371/journal.pone.0049531
1103 Hirota, J. and Szyper, J.P. (1975) Separation of total particulate carbon into inorganic and
1104 organic components1. *Limnology and Oceanography* 20, 896-900.
1105 doi:10.4319/lo.1975.20.5.0896
1106 Ingalls, A.E., Lee, C. and Druffel, E.R.M. (2003) Preservation of organic matter in mound-
1107 forming coral skeletons. *Geochim. Cosmochim. Acta* 67, 2827-2841. doi:10.1016/S0016-
1108 7037(03)00079-6
1109 Kast, E.R. (2020) Development and application of biogenic mineral-bound nitrogen isotope
1110 measurements to the million-year timescale, Geosciences Department. Princeton University,
1111 Princeton, NJ.
1112 Kast, E.R., Stolper, D.A., Auderset, A., Higgins, J.A., Ren, H., Wang, X.T., *et al.* (2019)
1113 Nitrogen isotope evidence for expanded ocean suboxia in the early Cenozoic. *Science* 364,
1114 386-389. doi:10.1126/science.aau5784
1115 Killingley, J.S. (1983) Effects of diagenetic recrystallization on $^{18}O/^{16}O$ values of deep-sea
1116 sediments. *Nature* 301, 594-597. doi:10.1038/301594a0
1117 Knapp, A.N., Sigman, D.M. and Lipschultz, F. (2005) N isotopic composition of dissolved
1118 organic nitrogen and nitrate at the Bermuda Atlantic time-series study site. *Global*
1119 *Biogeochemical Cycles* 19. doi:Artn Gb1018
1120 10.1029/2004gb002320
1121 Kroger, N. (2002) Self-Assembly of Highly Phosphorylated Silaffins and Their Function in
1122 Biosilica Morphogenesis. *Science* 298, 584-586. doi:10.1126/science.1076221
1123 Kroger, N., Deutzmann, R., Bergsdorf, C. and Sumper, M. (2000) Species-specific polyamines
1124 from diatoms control silica morphology. *Proceedings of the National Academy of Sciences* 97,
1125 14133-14138. doi:10.1073/pnas.260496497
1126 Kullmer, O. (2008) The fossil suidae from the Plio-Pleistocene Chiwondo Beds of northern
1127 Malawi, Africa. *Journal of Vertebrate Paleontology* 28, 208-216. doi:10.1671/0272-
1128 4634(2008)28[208:Tfsftp]2.0.Co;2
1129 Leichliter, J.N., Lüdecke, T., Foreman, A.D., Duprey, N.N., Winkler, D.E., Kast, E.R., *et al.*
1130 (2021) Nitrogen isotopes in tooth enamel record diet and trophic level enrichment: Results
1131 from a controlled feeding experiment. *Chemical Geology* 563, 120047.
1132 doi:10.1016/j.chemgeo.2020.120047
1133 Lueders-Dumont, J.A., Wang, X.T., Jensen, O.P., Sigman, D.M. and Ward, B.B. (2018) Nitrogen
1134 isotopic analysis of carbonate-bound organic matter in modern and fossil fish otoliths.
1135 *Geochim. Cosmochim. Acta* 224, 200-222. doi:10.1016/j.gca.2018.01.001
1136 Malinverno, A. and Martinez, E.A. (2015) The effect of temperature on organic carbon
1137 degradation in marine sediments. *Sci Rep* 5, 17861. doi:10.1038/srep17861
1138 Martinez-Garcia, A., Sigman, D.M., Ren, H.J., Anderson, R.F., Straub, M., Hodell, D.A., *et al.*
1139 (2014) Iron Fertilization of the Subantarctic Ocean During the Last Ice Age. *Science* 343,
1140 1347-1350. doi:10.1126/science.1246848
1141 McCorkle, D.C., Martin, P.A., Lea, D.W. and Klinkhammer, G.P. (1995) Evidence of a
1142 dissolution effect on benthic foraminiferal shell chemistry: $\delta^{13}C$, Cd/Ca, Ba/Ca, and Sr/Ca

results from the Ontong Java Plateau. *Paleoceanography* 10, 699-714. doi:10.1029/95pa01427

Mehra, O.P. and Jackson, M.L. (1958) Iron Oxide Removal from Soils and Clays by a Dithionite–Citrate System Buffered with Sodium Bicarbonate. *Clays and Clay Minerals* 7, 317-327. doi:10.1346/CCMN.1958.0070122

Morales, L.V., Sigman, D.M., Horn, M.G. and Robinson, R.S. (2013) Cleaning methods for the isotopic determination of diatom-bound nitrogen in non-fossil diatom frustules. *Limnol Oceanogr-Meth* 11, 101-112. doi:10.4319/lom.2013.11.101

Pearson, P.N. (2017) Oxygen Isotopes in Foraminifera: Overview and Historical Review. *The Paleontological Society Papers* 18, 1-38. doi:10.1017/s1089332600002539

Pearson, P.N., Ditchfield, P.W., Singano, J., Harcourt-Brown, K.G., Nicholas, C.J., Olsson, R.K.*, et al.* (2001) Warm tropical sea surface temperatures in the Late Cretaceous and Eocene epochs. *Nature* 413, 481-487. doi:10.1038/35097000

Pearson, P.N., van Dongen, B.E., Nicholas, C.J., Pancost, R.D., Schouten, S., Singano, J.M. and Wade, B.S. (2007) Stable warm tropical climate through the Eocene Epoch. *Geology* 35. doi:10.1130/g23175a.1

Rejebian, V.A., Harris, A.G. and Huebner, J.S. (1987) Conodont color and textural alteration: An index to regional metamorphism, contact metamorphism, and hydrothermal alteration. *Geological Society of America Bulletin* 99. doi:10.1130/0016-7606(1987)99<471:Ccataa>2.0.Co;2

Ren, H. (2010) Developement and paleoceanographic application of plancktonic foraminifera-bound nitrogen isotopes, Department of Geoscience. Princeton University, Princeton, NJ.

Ren, H., Sigman, D.M., Martínez-García, A., Anderson, R.F., Chen, M.-T., Ravelo, A.C.*, et al.* (2017) Impact of glacial/interglacial sea level change on the ocean nitrogen cycle. *Proceedings of the National Academy of Sciences* 114, E6759-E6766. doi:10.1073/pnas.1701315114

Ren, H., Sigman, D.M., Meckler, A.N., Plessen, B., Robinson, R.S., Rosenthal, Y. and Haug, G.H. (2009) Foraminiferal Isotope Evidence of Reduced Nitrogen Fixation in the Ice Age Atlantic Ocean. *Science* 323, 244-248. doi:10.1126/science.1165787

Ren, H.J., Brunelle, B.G., Sigman, D.M. and Robinson, R.S. (2013) Diagenetic aluminum uptake into diatom frustules and the preservation of diatom-bound organic nitrogen. *Mar. Chem.* 155, 92-101. doi:10.1016/j.marchem.2013.05.016

Ren, H.J., Studer, A.S., Serno, S., Sigman, D.M., Winckler, G., Anderson, R.F.*, et al.* (2015) Glacial-to-interglacial changes in nitrate supply and consumption in the subarctic North Pacific from microfossil-bound N isotopes at two trophic levels. *Paleoceanography* 30, 1217-1232. doi:10.1002/2014pa002765

Roach, D. and Gehrke, C.W. (1970) The hydrolysis of proteins. *Journal of Chromatography A* 52, 393-404. doi:10.1016/s0021-9673(01)96589-6

Robinson, J.R. and Kingston, J.D. (2020) Burned by the fire: Isotopic effects of experimental combustion of faunal tooth enamel. *Journal of Archaeological Science: Reports* 34. doi:10.1016/j.jasrep.2020.102593

Robinson, R.S., Brunelle, B.G. and Sigman, D.M. (2004) Revisiting nutrient utilization in the glacial Antarctic: Evidence from a new method for diatom-bound N isotopic analysis. *Paleoceanography* 19. doi:10.1029/2003pa000996

1187 Robinson, R.S., Kienast, M., Luiza Albuquerque, A., Altabet, M., Contreras, S., De Pol Holz, R.*, et al.* (2012) A review of nitrogen isotopic alteration in marine sediments. *Paleoceanography* 27. doi:10.1029/2012pa002321
1190 Robinson, R.S., Sigman, D.M., DiFiore, P.J., Rohde, M.M., Mashiotta, T.A. and Lea, D.W. (2005) Diatom-bound N-15/N-14: New support for enhanced nutrient consumption in the ice age subantarctic. *Paleoceanography* 20. doi:10.1029/2004pa001114
1193 Rosenthal, Y., Lohmann, G.P., Lohmann, K.C. and Sherrell, R.M. (2000) Incorporation and preservation of Mg inGlobigerinoides sacculifer:implications for reconstructing the temperature and $^{18}O/^{16}O$ of seawater. *Paleoceanography* 15, 135-145. doi:10.1029/1999pa000415
1197 Schroeder, R.A. (1975) Absence of β-alanine and γ-aminobutyric acid in cleaned foraminiferal shells: Implications for use as a chemical criterion to indicate removal of non-indigenous amino acid contaminants. *Earth Planet. Sci. Lett.* 25, 274-278. doi:10.1016/0012-821x(75)90241-1
1201 Shemesh, A., Macko, S.A., Charles, C.D. and Rau, G.H. (1993) Isotopic Evidence for Reduced Productivity in the Glacial Southern Ocean. *Science* 262, 407-410. doi:10.1126/science.262.5132.407
1204 Shipman, P., Foster, G. and Schoeninger, M. (1984) Burnt Bones and Teeth - an Experimental-Study of Color, Morphology, Crystal-Structure and Shrinkage. *J Archaeol Sci* 11, 307-325. doi:Doi 10.1016/0305-4403(84)90013-X
1207 Sigman, D.M., Altabet, M.A., Francois, R., McCorkle, D.C. and Gaillard, J.F. (1999) The isotopic composition of diatom-bound nitrogen in Southern Ocean sediments. *Paleoceanography* 14, 118-134. doi:Doi 10.1029/1998pa900018
1210 Sigman, D.M., Casciotti, K.L., Andreani, M., Barford, C., Galanter, M. and Bohlke, J.K. (2001) A bacterial method for the nitrogen isotopic analysis of nitrate in seawater and freshwater. *Analytical Chemistry* 73, 4145-4153. doi:DOI 10.1021/ac010088e
1213 Sigman, D.M. and Fripiat, F. (2019) Nitrogen Isotopes in the Ocean, Encyclopedia of Ocean Sciences, pp. 263-278.
1215 Sigman, D.M., Fripiat, F., Studer, A.S., Kemeny, P.C., Martínez-García, A., Hain, M.P.*, et al.* (2021) The Southern Ocean during the ice ages: A review of the Antarctic surface isolation hypothesis, with comparison to the North Pacific. *Quat. Sci. Rev.* 254, 106732. doi:10.1016/j.quascirev.2020.106732
1219 Smart, S.M., Ren, H., Fawcett, S.E., Schiebel, R., Conte, M., Rafter, P.A.*, et al.* (2018) Ground-truthing the planktic foraminifer-bound nitrogen isotope paleo-proxy in the Sargasso Sea. *Geochim. Cosmochim. Acta* 235, 463-482. doi:10.1016/j.gca.2018.05.023
1222 Smith, A.C., Leng, M.J., Swann, G.E.A., Barker, P.A., Mackay, A.W., Ryves, D.B.*, et al.* (2016) An experiment to assess the effects of diatom dissolution on oxygen isotope ratios. *Rapid Commun. Mass Spectrom.* 30, 293-300. doi:10.1002/rcm.7446
1225 Stolarski, J. (2003) Three-dimensional micro- and nanostructural characteristics of the scleractinian coral skeleton: A biocalcification proxy. *Acta Palaeontol Pol* 48, 497-530.
1227 Straub, M. (2012) Application of foraminifera-bound nitrogen isotopes to Atlantic paleoceanography, Earth Science Department. ETH Zurich, Zurich.
1229 Straub, M., Sigman, D.M., Auderset, A., Ollivier, J., Petit, B., Hinnenberg, B.*, et al.* (2021) Distinct nitrogen isotopic compositions of healthy and cancerous tissue in mice brain and head&neck micro-biopsies. *BMC Cancer* 21, 805. doi:10.1186/s12885-021-08489-x

1232 Straub, M., Sigman, D.M., Ren, H., Martinez-Garcia, A., Meckler, A.N., Hain, M.P. and Haug,
1233 G.H. (2013) Changes in North Atlantic nitrogen fixation controlled by ocean circulation.
1234 *Nature* 501, 200-203. doi:10.1038/nature12397
1235 Studer, A.S., Martinez-Garcia, A., Jaccard, S.L., Girault, F.E., Sigman, D.M. and Haug, G.H.
1236 (2012) Enhanced stratification and seasonality in the Subarctic Pacific upon Northern
1237 Hemisphere Glaciation-New evidence from diatom-bound nitrogen isotopes, alkenones and
1238 archaeal tetraethers. *Earth Planet. Sci. Lett.* 351, 84-94. doi:10.1016/j.epsl.2012.07.029
1239 Studer, A.S., Mekik, F., Ren, H., Hain, M.P., Oleynik, S., Martínez-García, A.*, et al.* (2021) Ice
1240 Age-Holocene Similarity of Foraminifera-Bound Nitrogen Isotope Ratios in the Eastern
1241 Equatorial Pacific. *Paleoceanography and Paleoclimatology* 36. doi:10.1029/2020pa004063
1242 Studer, A.S., Sigman, D.M., Martinez-Garcia, A., Benz, V., Winckler, G., Kuhn, G.*, et al.* (2015)
1243 Antarctic Zone nutrient conditions during the last two glacial cycles. *Paleoceanography* 30,
1244 845-862. doi:10.1002/2014PA002745
1245 Studer, A.S., Sigman, D.M., Martínez-García, A., Thöle, L.M., Michel, E., Jaccard, S.L.*, et al.*
1246 (2018) Increased nutrient supply to the Southern Ocean during the Holocene and its
1247 implications for the pre-industrial atmospheric CO_2 rise. *Nat Geosci* 11, 756-760.
1248 doi:10.1038/s41561-018-0191-8
1249 Sulpis, O., Jeansson, E., Dinauer, A., Lauvset, S.K. and Middelburg, J.J. (2021) Calcium
1250 carbonate dissolution patterns in the ocean. *Nat Geosci* 14, 423-428. doi:10.1038/s41561-021-
1251 00743-y
1252 Swart, K.A., Oleynik, S., Martínez-García, A., Haug, G.H. and Sigman, D.M. (2021) Correlation
1253 between the carbon isotopic composition of planktonic foraminifera-bound organic matter and
1254 surface water pCO_2 across the equatorial Pacific. *Geochim. Cosmochim. Acta* 306, 281-303.
1255 doi:10.1016/j.gca.2021.03.007
1256 Tomiak, P.J., Penkman, K.E.H., Hendy, E.J., Demarchi, B., Murrells, S., Davis, S.A.*, et al.*
1257 (2013) Testing the limitations of artificial protein degradation kinetics using known-age
1258 massive Porites coral skeletons. *Quat Geochronol* 16, 87-109.
1259 doi:10.1016/j.quageo.2012.07.001
1260 Van Cappellen, P., Dixit, S. and van Beusekom, J. (2002) Biogenic silica dissolution in the
1261 oceans: Reconciling experimental and field-based dissolution rates. *Global Biogeochemical*
1262 *Cycles* 16, 23-21-23-10. doi:10.1029/2001gb001431
1263 Van Eynde, E., Lenaerts, B., Tytgat, T., Verbruggen, S.W., Hauchecorne, B., Blust, R. and
1264 Lenaerts, S. (2014) Effect of pretreatment and temperature on the properties of Pinnularia
1265 biosilica frustules. *RSC Adv.* 4, 56200-56206. doi:10.1039/c4ra09305d
1266 Wang, X.C.T., Prokopenko, M.G., Sigman, D.M., Adkins, J.F., Robinson, L.F., Ren, H.J.*, et al.*
1267 (2014) Isotopic composition of carbonate-bound organic nitrogen in deep-sea scleractinian
1268 corals: A new window into past biogeochemical change. *Earth Planet. Sci. Lett.* 400, 243-250.
1269 doi:10.1016/j.epsl.2014.05.048
1270 Wang, X.T., Sigman, D.M., Cohen, A.L., Sinclair, D.J., Sherrell, R.M., Cobb, K.M.*, et al.* (2016)
1271 Influence of open ocean nitrogen supply on the skeletal delta N-15 of modern shallow-water
1272 scleractinian corals. *Earth Planet. Sci. Lett.* 441, 125-132. doi:10.1016/j.epsl.2016.02.032
1273 Wang, X.T., Sigman, D.M., Prokopenko, M.G., Adkins, J.F., Robinson, L.F., Hines, S.K.*, et al.*
1274 (2017) Deep-sea coral evidence for lower Southern Ocean surface nitrate concentrations
1275 during the last ice age. *Proceedings of the National Academy of Sciences of the United States*
1276 *of America* 114, 3352-3357. doi:10.1073/pnas.1615718114

1277 Weigand, M.A., Foriel, J., Barnett, B., Oleynik, S. and Sigman, D.M. (2016) Updates to
1278 instrumentation and protocols for isotopic analysis of nitrate by the denitrifier method. *Rapid*
1279 *Commun. Mass Spectrom.* 30, 1365-1383. doi:10.1002/rcm.7570
1280 Weiner, S. and Erez, J. (1984) Organic matrix of the shell of the foraminifer, Heterostegina
1281 depressa. *The Journal of Foraminiferal Research* 14, 206-212. doi:10.2113/gsjfr.14.3.206
1282 Weiss, I.M., Muth, C., Drumm, R. and Kirchner, H.O.K. (2018) Thermal decomposition of the
1283 amino acids glycine, cysteine, aspartic acid, asparagine, glutamic acid, glutamine, arginine
1284 and histidine. *BMC Biophysics* 11. doi:10.1186/s13628-018-0042-4
1285 Whelan, J.K. (1977) Amino acids in a surface sediment core of the Atlantic abyssal plain.
1286 *Geochim. Cosmochim. Acta* 41, 803-810. doi:10.1016/0016-7037(77)90050-3
1287 Wolf, N., Carleton, S.A. and Martínez del Rio, C. (2009) Ten years of experimental animal
1288 isotopic ecology. *Functional Ecology* 23, 17-26. doi:10.1111/j.1365-2435.2009.01529.x
1289 Yoshioka, S. and Kitano, Y. (1985) Transformation of aragonite to calcite through heating.
1290 *Geochem J* 19, 245-249. doi:10.2343/geochemj.19.245
1291 Zheng, Y., Anderson, R.F., Froelich, P.N., Beck, W., McNichol, A.P. and Guilderson, T. (2002)
1292 Challenges in Radiocarbon Dating Organic Carbon in Opal-Rich Marine Sediments.
1293 *Radiocarbon* 44, 123-136. doi:10.1017/s0033822200064729
1294

Figure 1.

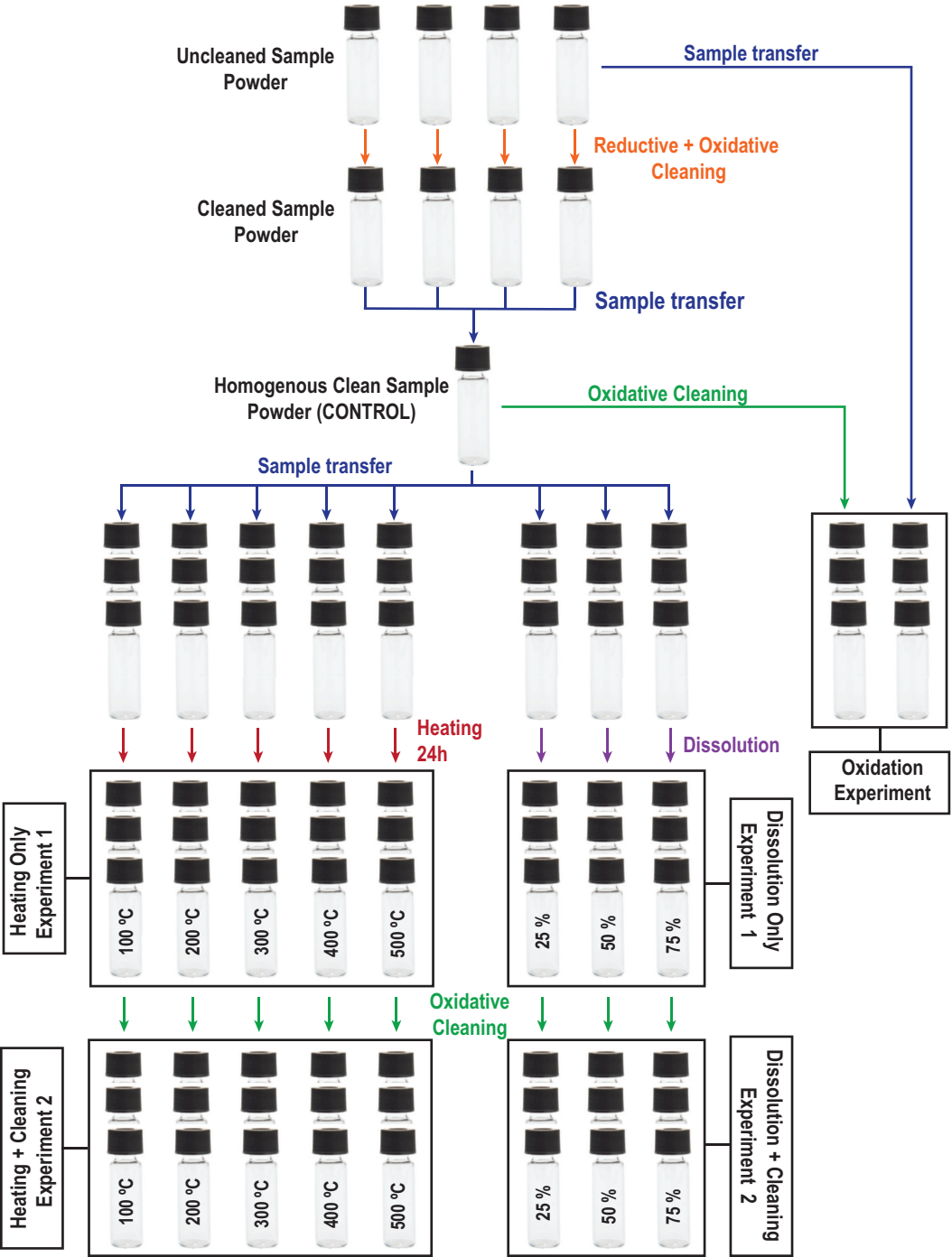
Uncleaned Sample Powder
Sample transfer
Reductive + Oxidative Cleaning
Cleaned Sample Powder
Sample transfer
Homogenous Clean Sample Powder (CONTROL)
Oxidative Cleaning
Sample transfer
Heating 24h
Dissolution
Oxidation Experiment
Heating Only Experiment 1
100 °C
200 °C
300 °C
400 °C
500 °C
25 %
50 %
75 %
Dissolution Only Experiment 1
Oxidative Cleaning
Heating + Cleaning Experiment 2
100 °C
200 °C
300 °C
400 °C
500 °C
25 %
50 %
75 %
Dissolution + Cleaning Experiment 2

Figure 2.

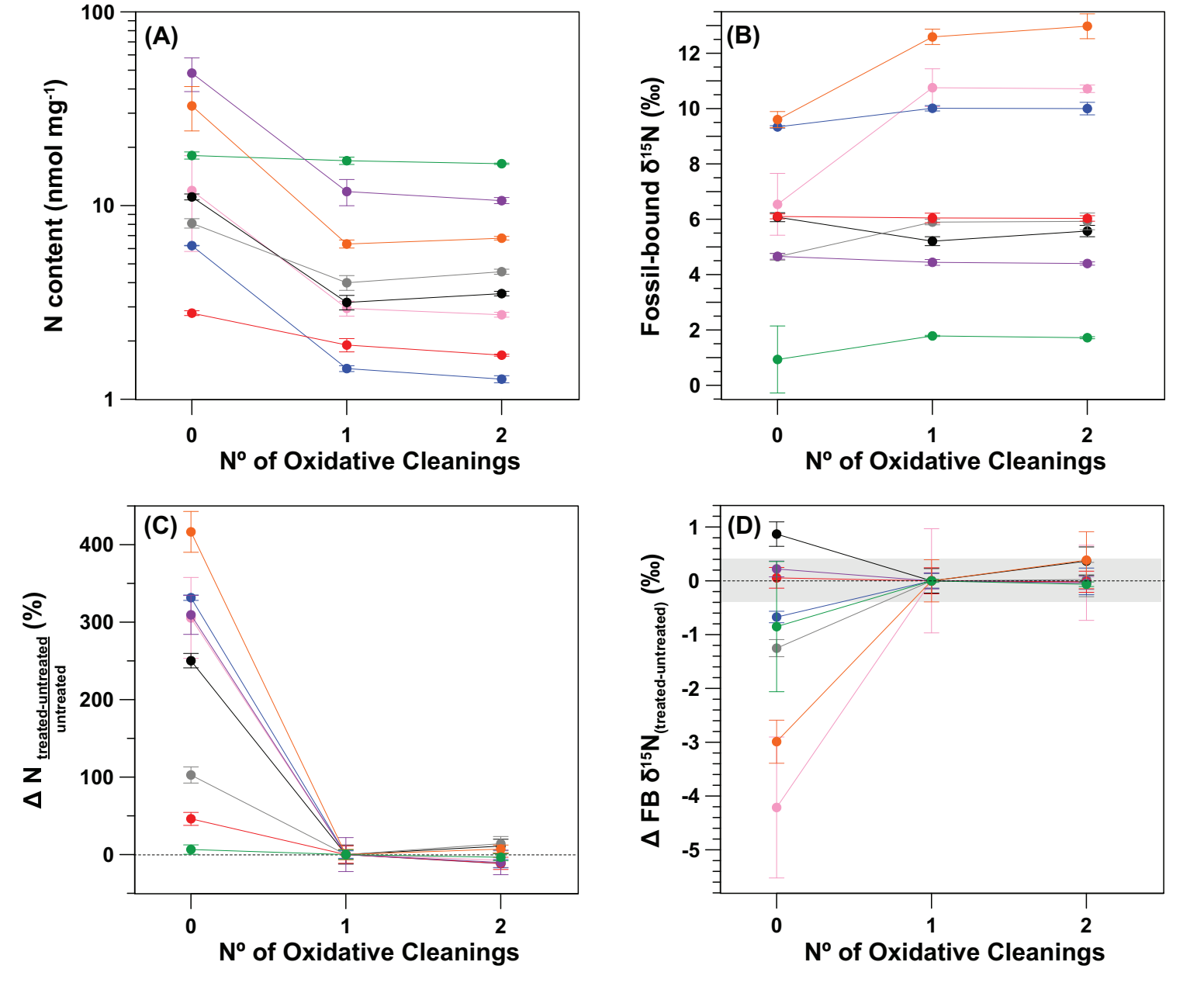

LO-1 (Deep sea coral, *Lophelia sp.*)
PO-1 (Shallow water coral, *Porites sp.*)
Di-1 (Diatoms, Southern Ocean)
MF-1(Mix. Foraminifera, North Atlantic)
MF-2 (Mix. Foraminifera, Southern Ocean)
AG-lox (Modern enamel, *Loxodonta africana*)
Noto-2 (Fossil enamel, *Notochoerus scotti*)
Hippo-1 (Fossil enamel, *Hippopotamus amphibius*)

Figure 3.

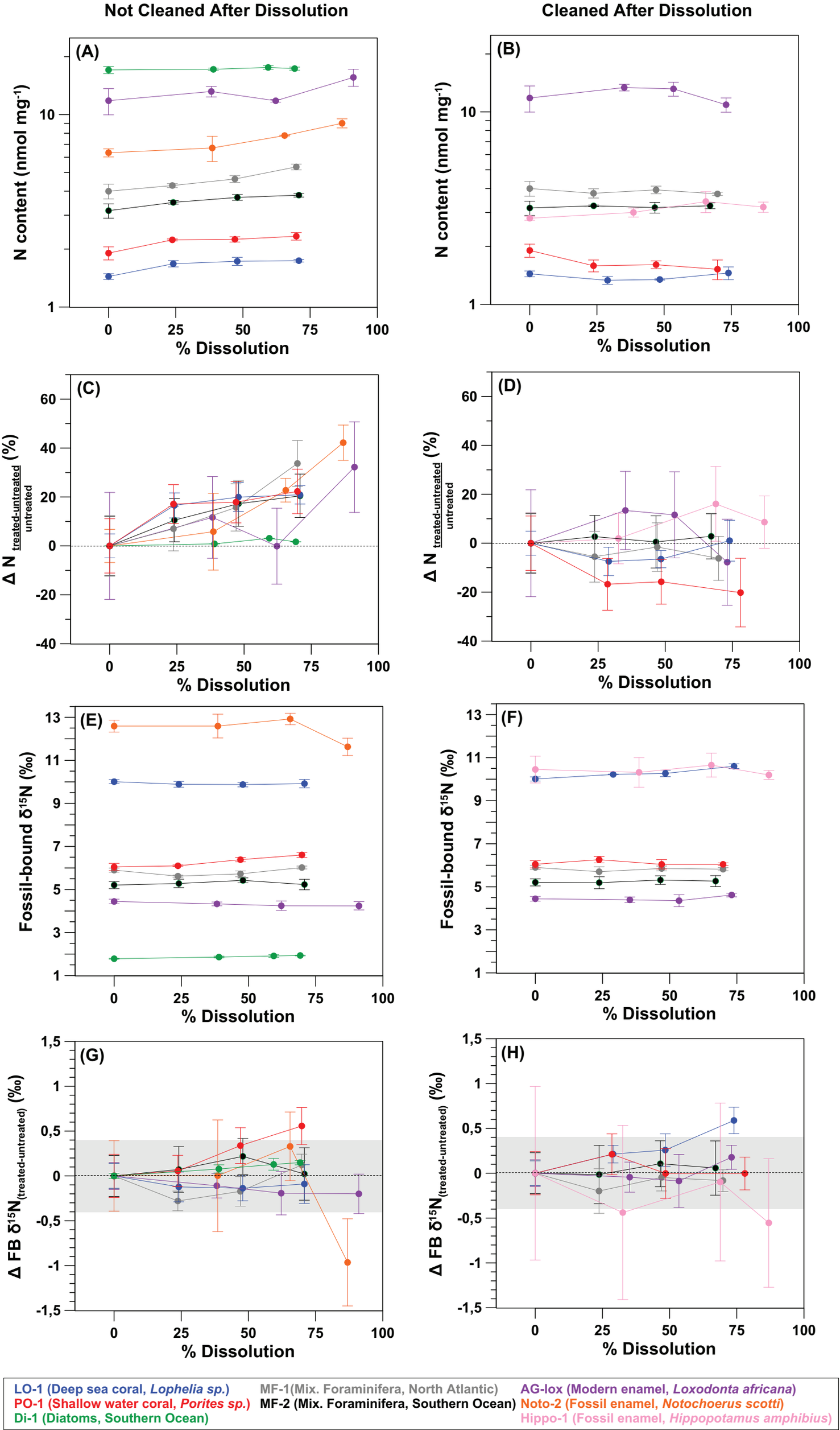
Not Cleaned After Dissolution
Cleaned After Dissolution
(A)
(B)
(C)
(D)
(E)
(F)
(G)
(H)
N content (nmol mg-1)
Δ N treated-untreated / untreated (%)
Fossil-bound δ15N (‰)
Δ FB δ15N(treated-untreated) (‰)
% Dissolution
LO-1 (Deep sea coral, Lophelia sp.)
PO-1 (Shallow water coral, Porites sp.)
Di-1 (Diatoms, Southern Ocean)
MF-1(Mix. Foraminifera, North Atlantic)
MF-2 (Mix. Foraminifera, Southern Ocean)
AG-lox (Modern enamel, Loxodonta africana)
Noto-2 (Fossil enamel, Notochoerus scotti)
Hippo-1 (Fossil enamel, Hippopotamus amphibius)

Figure 4.

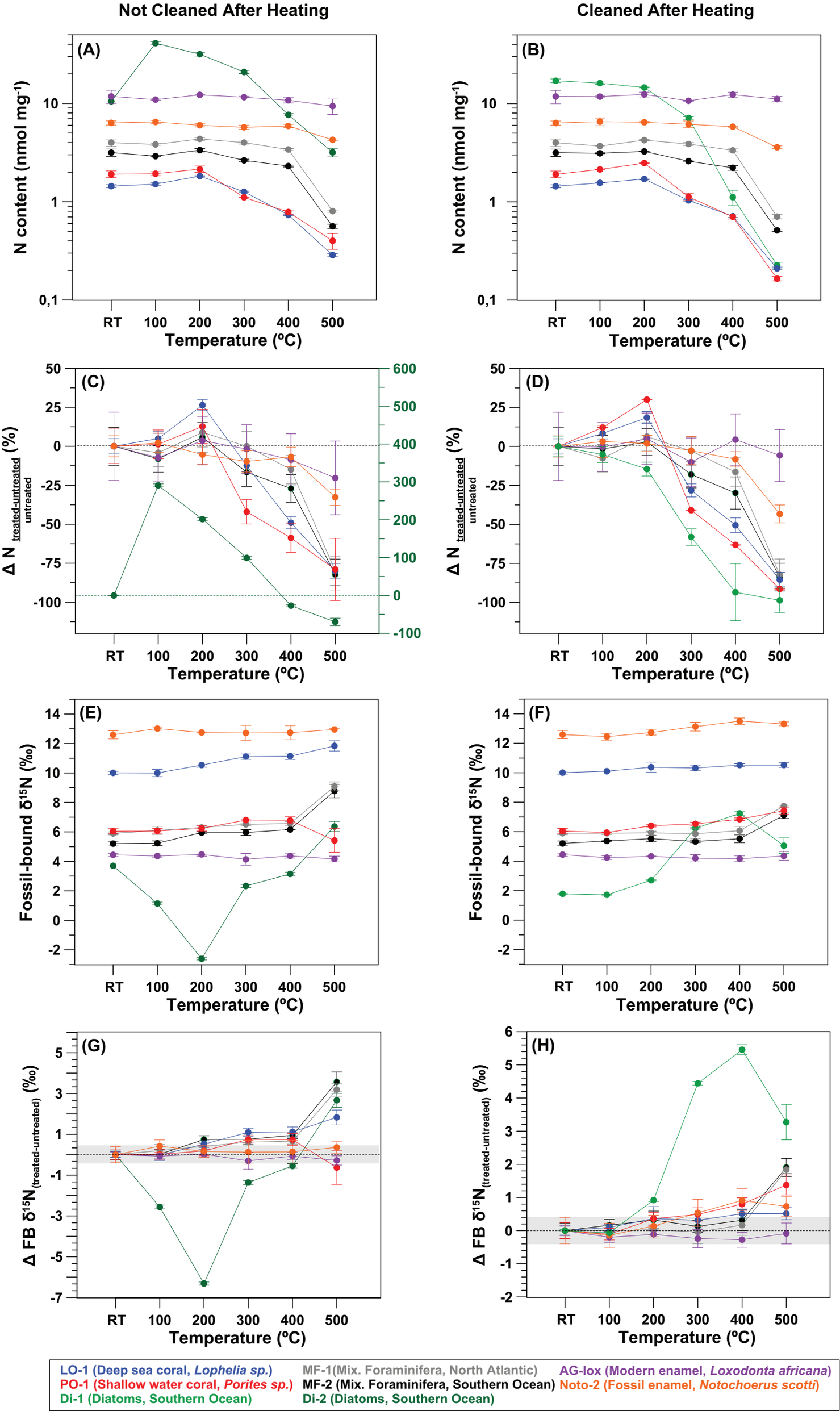
Not Cleaned After Heating
Cleaned After Heating
(A)
(B)
N content (nmol mg-1)
Temperature (ºC)
RT
100
200
300
400
500
(C)
(D)
Δ N treated-untreated / untreated (%)
(E)
(F)
Fossil-bound δ15N (‰)
(G)
(H)
Δ FB δ15N(treated-untreated) (‰)
LO-1 (Deep sea coral, Lophelia sp.)
PO-1 (Shallow water coral, Porites sp.)
Di-1 (Diatoms, Southern Ocean)
MF-1(Mix. Foraminifera, North Atlantic)
MF-2 (Mix. Foraminifera, Southern Ocean)
Di-2 (Diatoms, Southern Ocean)
AG-lox (Modern enamel, Loxodonta africana)
Noto-2 (Fossil enamel, Notochoerus scotti)

Figure 5.

Not Cleaned After Heating

RT - 500ºC

LO-1 ε = -0.89‰, r^2 = 0.72 | PO-1 ε = 0.21‰, r^2 = 0.07
FM-1 ε = -1.76‰, r^2 = 0.97 | FM-2 ε = -1.22‰, r^2 = 0.88
AGLox ε = 0.84‰, r^2 = 0.32 | Noto-1 ε = -0.37‰, r^2 = 0.13
DI-2 ε = -2.63‰, r^2 = 0.72

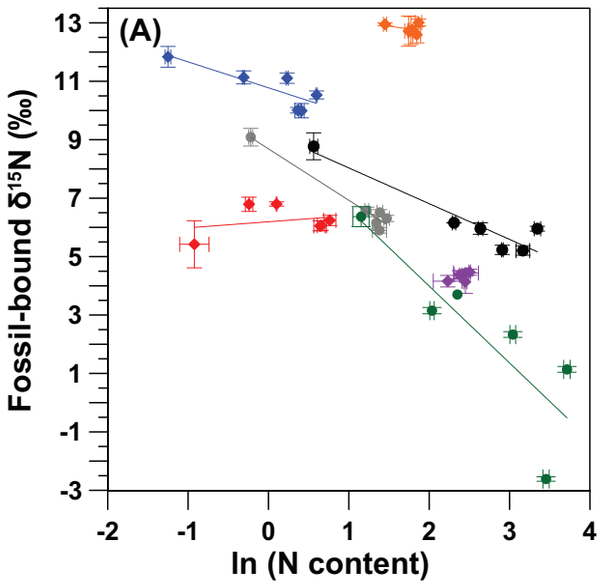

RT - 400ºC

LO-1 ε = -1.04‰, r^2 = 0.41 | PO-1 ε = -0.80‰, r^2 = 0.83
FM-1 ε = -1.14‰, r^2 = 0.14 | FM-2 ε = -0.52‰, r^2 = 0.24
AGLox ε = 0.44‰, r^2 = 0.03 | Noto-1 ε = 1.20‰, r^2 = 0.16
DI-2 ε = -2.5‰, r^2 = 0.50

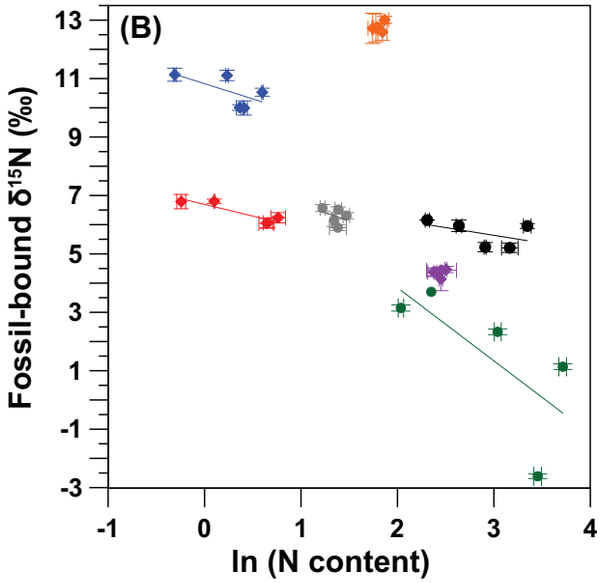

RT - 300ºC

LO-1 ε = -1.21‰, r^2 = 0.12 | PO-1 ε = -1.08‰, r^2 = 0.83
FM-1 ε = 1.30‰, r^2 = 0.07 | M-2 ε = -0.14‰, r^2 = 0.01
AGLox ε = 0.96‰, r^2 = 0.09 | Noto-1 ε = 1.23‰, r^2 = 0.15
DI-2 ε = -3.13‰, r^2 = 0.47

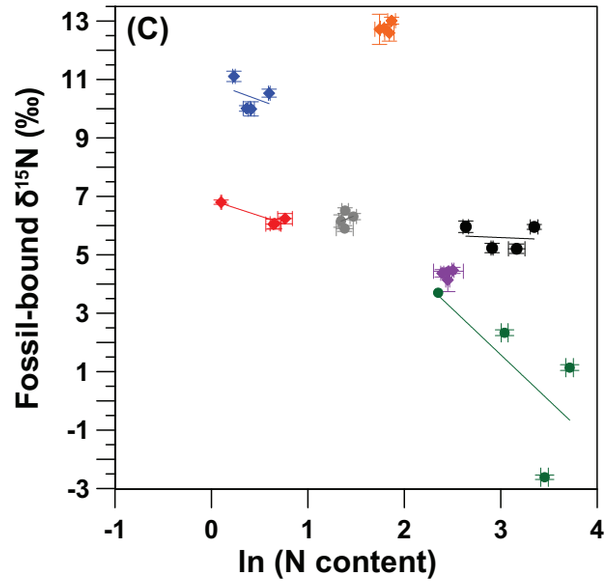

Cleaned After Heating

RT - 500ºC

LO-1 ε = -0.18‰, r^2 = 0.47 | PO-1 ε = -0.50‰, r^2 = 0.87
FM-1 ε = -1.06‰, r^2 = 0.99 | FM-2 ε = -0.64‰, r^2 = 0.87
AGLox ε = 0.03‰, r^2 = 0.00 | Noto-1 ε = -1.06‰, r^2 = 0.33
DI-1 ε = -0.91‰, r^2 = 0.45

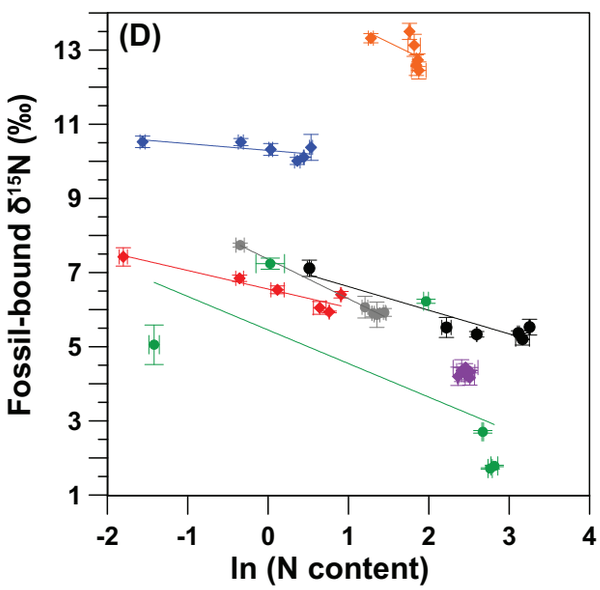

RT - 400ºC

LO-1 ε = -0.37‰, r^2 = 0.42 | PO-1 ε = -0.57‰, r^2 = 0.65
FM-1 ε = -0.61‰, r^2 = 0.48 | FM-2 ε = -0.10‰, r^2 = 0.10
AGLox ε = 0.2 ‰, r^2 = 0.02 | Noto-1 ε = -8.90‰, r^2 = 0.91
DI-1 ε = -1.94‰, r^2 = 0.78

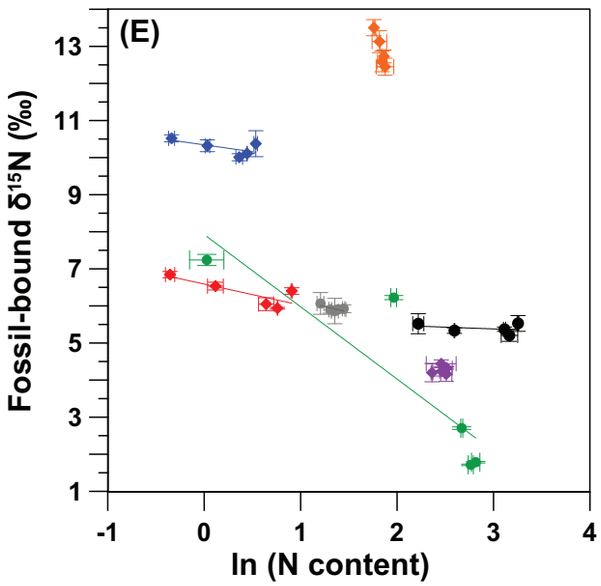

RT - 300ºC

LO-1 ε = -0.12‰, r^2 = 0.02 | PO-1 ε = -0.42‰, r^2 = 0.26
FM-1 ε = 0.27‰, r^2 = 0.34 | FM-2 ε = 0.11‰, r^2 = 0.06
AGlox ε = 0.87‰, r^2 = 0.27 | Noto-1 ε = -10.02‰, r^2 = 0.76
DI-1 ε = -5.33‰, r^2 = 0.99

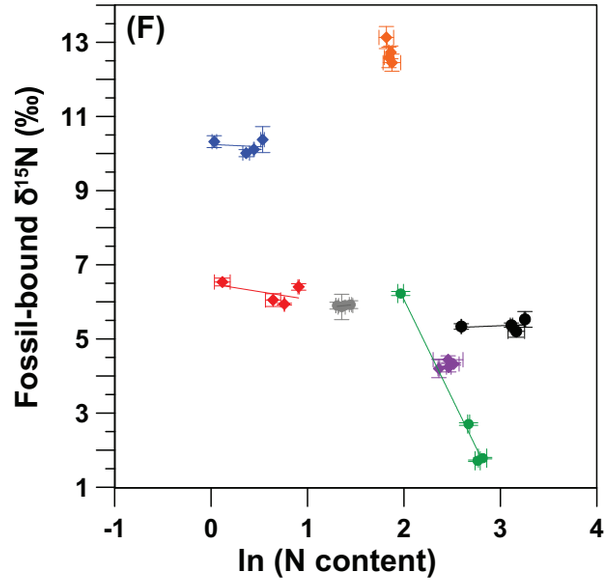

LO-1 (Deep sea coral, *Lophelia sp.*) | MF-1(Mix. Foraminifera, North Atlantic) | AG-lox (Modern enamel, *Loxodonta africana*)
PO-1 (Shallow water coral, *Porites sp.*) | MF-2 (Mix. Foraminifera, Southern Ocean) | Noto-2 (Fossil enamel, *Notochoerus scotti*)
Di-1 (Diatoms, Southern Ocean) | Di-2 (Diatoms, Southern Ocean)

Figure 6.

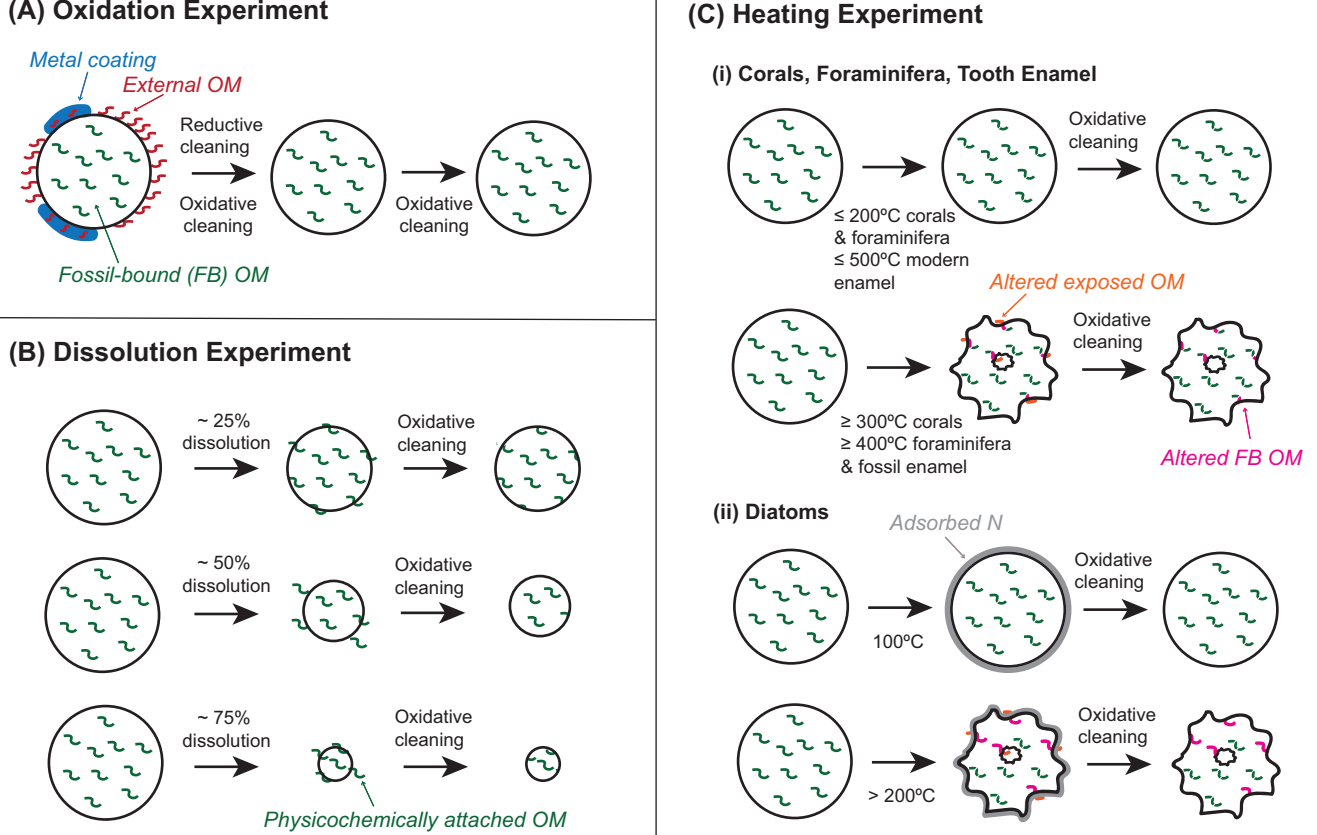
(A) Oxidation Experiment
Metal coating
External OM
Reductive cleaning
Oxidative cleaning
Oxidative cleaning
Fossil-bound (FB) OM
(B) Dissolution Experiment
~ 25% dissolution
Oxidative cleaning
~ 50% dissolution
Oxidative cleaning
~ 75% dissolution
Oxidative cleaning
Physicochemically attached OM
(C) Heating Experiment
(i) Corals, Foraminifera, Tooth Enamel
Oxidative cleaning
≤ 200ºC corals & foraminifera ≤ 500ºC modern enamel
Altered exposed OM
Oxidative cleaning
≥ 300ºC corals ≥ 400ºC foraminifera & fossil enamel
Altered FB OM
(ii) Diatoms
Adsorbed N
Oxidative cleaning
100ºC
Oxidative cleaning
> 200ºC